UNIVERSITY OF OKLAHOMA

GRADUATE COLLEGE

IEEE 802.11AC PERFORMANCE ANALYSIS AND MEASUREMENT TOOLS

A THESIS

SUBMITTED TO THE GRADUATE FACULTY

in partial fulfillment of the requirements for the

Degree of

MASTER OF SCIENCE

By

MADELENE GHANEM
Norman, Oklahoma
2018

Downloaded from SHAREOK. Persistent Handle URL: https://hdl.handle.net/11244/301378

IEEE 802.11AC PERFORMANCE ANALYSIS AND MEASUREMENT TOOLS

A THESIS APPROVED FOR THE
SCHOOL OF ELECTRICAL AND COMPUTER ENGINEERING

BY

_____
Dr. Hazem Refai, Chair

_____
Dr. Thordur Runolfsson

_____
Dr. Ali Imran

© Copyright by MADELENE GHANEM 2018
All Rights Reserved.

To my beloved parents, Noura and Mohammed, who have been loving, inspiring, and supporting in every way in every step of the road.

To my dear siblings and their families for believing in and supporting me.

To all my friends who stood by me and encouraged me.

I thank you and dedicate this work to you.

Madelene Ghanem

Acknowledgments

I would like to extend my heartfelt appreciation and gratitude to my advisor, *Dr. Hazem H. Refai*, for the support and guidance he has provided throughout my Master Degree journey at The University of Oklahoma.

I would also like to express my sincere gratitude to the distinguished members of my thesis committee. *Dr. Thordur Runolfsson*, and *Dr. Ali Imran.* Thank you all.

I must acknowledge all my fellow students who inspired, encouraged, and supported me unconditionally and without any hesitance.

Special appreciation goes to the OU-TULSA family of professors, students, and staff.

Table of Contents

Acknowledgments iv

List of Tables vii

List of Figures viii

Abstract x

Chapter 1: Introduction 1

Contributions 2

Chapter 2 – Background 4

Related Work 4

Spectrum Surveys measurement tools 4

Performance analysis of IEEE 802.11 Standard 6

Chapter 3 – Software Development for Long-Term Surveys 9

PESA Implementation 9

Methodology 9

Hardware 12

Experimental Results 13

Discussion 16

Chapter 4 – IEEE 802.11ac Performance Analysis 18

IEEE 802.11ac Standard 18

PHY and MAC Layer Enhancements 19

Experimental Setup 21

Experimental Results 23

Throughput Analysis without the Interference 23

Throughput Analysis with the Interference 35
Delay Analysis 37
Discussion 40
Chapter 5 - Conclusion and Future Work 43
Conclusion 43
Future work 44
References 45
Appendix A 48

List of Tables

Table 1. Statistics of the IEEE 802.11ac throughput model for UDP Protocol. 26

Table 2. Coefficients of the logarithmic model of the IEEE 802.11ac throughput. 28

Table 3. Statistics of the logarithmic model of the IEEE 802.11ac throughput. 28

Table 4. Statistics of the IEEE 802.11ac throughput model for TCP Protocol. 30

Table 5. Statistics of the IEEE 802.11ac delay model. 38

Table 6. Coefficients of the IEEE 802.11ac delay model. 38

List of Figures

Figure 1. PESA System Processing Flow. 10

Figure 2. Comparison of the storage volume between the original power samples and the PESA output CSV files. The data generated from the survey was saved into 25 16-minute long separate files. 14

Figure 3. Comparison between the original power measurements and the regenerated ones using PESA. 15

Figure 4. The fitted PDF of the Channel Utilization calculated using PESA output. 16

Figure 5. IEEE 802.11 Maximum Theoretical Data Rates. 18

Figure 6. The channelization in the IEEE 802.11ac standard. 19

Figure 7. The channel-list elements for 802.11ac. a) 40 MHz, 80 MHz, and 160 MHz channel width. b) 80+80 MHz channel width. 20

Figure 8. VHT PPDU Format. 21

Figure 9. MAC Frame Format. 21

Figure 10. IEEE 802.11ac Measurement Setup. 21

Figure 11. Mikrotik router boards 953GS-5HnT-RP with R11e-5HacD wireless card. 22

Figure 12. Comparison of throughput vs SNR for different channel bandwidths for UDP Protocol and two spatial streams. 24

Figure 13. IEEE 802.11ac throughput vs SNR model for UDP Protocol and two spatial streams. a) 20 MHz channel width. b) 40 MHz channel width. c) 80 MHz channel width. 27

Figure 14. IEEE 802.11ac throughput vs SNR logarithmic model for UDP Protocol and two spatial streams. a) 20 MHz channel width. b) 40 MHz channel width. c) 80 MHz channel width..... 30
Figure 15. Comparison of throughput vs SNR for different channel bandwidths for TCP Protocol and two spatial streams. 31
Figure 16. IEEE 802.11ac throughput vs SNR model for TCP Protocol and two spatial streams. a) 20 MHz channel width. b) 40 MHz channel width. c) 80 MHz channel width. 32
Figure 17. Comparison between the throughput of IEEE 802.11ac with 80MHz channel bandwidth for UDP and TCP Protocols a) One spatial stream. b) Two spatial streams. 34
Figure 18. Comparison between the throughput of IEEE 802.11ac with 80MHz channel bandwidth when using one spatial stream and two spatial streams for UDP Protocol. . 34
Figure 19. The measurement Setup in the presence of the interfering network. 36
Figure 20. Comparison between the throughput of the IEEE 802.11ac DUT network and the Interfering network. 36
Figure 21. Comparison of Delay vs SNR for different channel bandwidths..... 37
Figure 22. IEEE 802.11ac delay vs SNR model. a) 20 MHz channel width. b) 40 MHz channel width. c) 80 MHz channel width. 39

Abstract

Wireless local area networks have witnessed a large growth over the course of the last decade which has led to increased data traffic and demand for higher speeds. One of the IEEE 802.11 standards family that was developed to offer very high throughput WLANs is IEEE 802.11ac. Theoretically, with the PHY and MAC enhancements embedded in this standard, it is expected to provide gigabit-per-second data rates.

The WLAN standards in addition to other wireless technologies such as Bluetooth and ZigBee share the same unlicensed band, and the increase in the use of this band requires monitoring the wireless spectrum and addressing wireless coexistence problems via spectrum surveys which usually produce a large data volume, that requires advanced hardware capabilities to help overcome the challenges of storing, retrieving and processing the data.

This thesis reports on the performance analysis of an IEEE 802.11ac network with respect to varied channel conditions such as SNR and SIR. Mathematical models of the relationship between the throughput, the delay of the network and SNR using interpolation, were provided. The results show that for good channel conditions i.e. high SNR, 802.11ac offers high throughput values. However, the throughput is highly affected by the interference level caused by other 802.11ac devices that share the same channel, as the throughput of the under-test network is directly proportional to the level of SIR.

Moreover, this thesis details a measurement tool that implements a probabilistic efficient storage algorithm (PESA) proposed by Dr. Al-Kalaa with US FDA that could

be used in deploying long-term spectrum surveys in the time-domain using LabVIEW. PESA algorithm is based on representing the dynamic range of a monitoring device by a Gaussian Mixture Model, establishing windows of activity and inactivity and mapping the windows to the Gaussian component with the largest responsibility for each window mean. The indexes of the Gaussian components are stored in addition to the count of samples in each window resulting in a significant storage volume reduction. The software was used to survey the 2.4 GHz band in a healthcare facility for 7 hours. The results show a reduction in the required storage size of approximately 98.8% while maintaining an accurate estimation of the channel utilization.

Chapter 1: Introduction

Wireless local area networks (WLANs) have a great impact on our daily life as they have been heavily deployed in businesses and residences. The tremendous growth of the deployment and popularity of wireless networks resulted in an increase in the demand for higher capacity, data rates, and quality of service. Hence, the need to enhance the PHY and MAC of the IEEE 802.11 network standards that are the base of the WLANs.

IEEE 802.11ac was published in 2013 as a very high throughput (VHT) WLAN standard that operates in the 5 GHz band. It further extends the basic features integrated in the 802.11n standard such as Multiple Input, Multiple Output (MIMO), channel bonding and higher modulation and coding schemes. It expands the channel bandwidth to 80 and 160 MHz using contiguous and non-contiguous channels; it offers a higher number of spatial streams up to 8, and it offers the ability to use 256-QAM modulation to achieve higher data rates. Furthermore, it enables multi-user MIMO to improve the network capacity by allowing multiple users to transmit simultaneously. Although the 802.11ac standard specifies a theoretical maximum throughput, the practical achievable throughput is highly affected by the channel conditions. There are multiple factors that could affect the performance of the 802.11ac wireless network such as the received signal power level, the nodes' distribution, the type of traffic, and the power received from interference sources.

An extensive amount of the literature has focused on performance studies for WLAN standards [13-22]. Some of the 802.11ac studies found in the literature were focused on simulating the network [21-22] while the other focused on analyzing the

performance of the network in a measurement-based study. However, the measurement-based studies were lacking as they only examined the effect of the distance on the throughput of the 802.11ac network. The effect of important QoS metrics such as SNR and SIR was not investigated. Moreover, no delay analysis was provided nor mathematical models were provided.

Contributions

The first half of the research reports on the development of a spectrum utilization measurement tool that implements the probabilistic efficient storage algorithm (PESA) [1] in real-time. The motivation behind this algorithm is facilitating the implementation of spectrum surveys which are useful for coexistence management and spectrum sharing. It helps monitoring the wireless environment and defining the interference sources and levels over the area of interest in a specific frequency band and build an interference map [2]. Spectrum Analyzers are used to monitor the wireless medium and acquire the power values observed in the intended environment. Reducing the amount of data generated by the spectrum survey measurements is a challenging task. The use of metrics to change the measurements into more meaningful data such as channel utilization has been widely used [2]. PESA algorithm aims to reduce the storage volume of the data produced by the IEEE 802.11 time-domain spectrum measurements while maintaining an accurate channel utilization estimation and signal temporal distributions.

The second half of this research reports on the analysis of the performance of the 802.11ac network where the performance indexes i.e. the throughput and the delay have been studied experimentally and mathematical models based on the empirical data were

introduced in this thesis. These models describe the relationship between the levels of signal to noise ratio (SNR) and the throughput and the delay. Moreover, the impact of the signal to interference ratio (SIR) on the throughput was examined.

This thesis is organized, as follows. A literature review of the related works studying the measurement tools used during spectrum surveys and the performance analysis of the IEEE 802.11 standards family are detailed in Chapter 2. Chapter 3 demonstrates the implementation of the probabilistic efficient storage algorithm (PESA) in addition to the validation and the experimental results of a 7-hour survey in a clinic environment. An experimental study to analyze the performance metrics of an IEEE 802.11ac network with respect to varied channel conditions and the experimental results are presented in Chapter 4. Chapter 5 concludes the thesis and details potential future works.

Chapter 2 – Background

Related Work

Spectrum Surveys measurement tools

Spectrum Sensing is one of the most important tasks for many wireless communication applications such as wireless coexistence in the industrial, scientific and medical (ISM) band and cognitive radio. It allows us to obtain information about the existence of the activity on the wireless channel and its pattern, as well as the utilization of the spectrum. Moreover, it enables coexistence-related purposes such as the development of coexistence management methods, spectrum sharing, and interference management. Due to the need for spectrum surveys and spectrum survey tools development, researchers in a wide range of fields have reported their contribution in the literature. For example, a survey of spectrum sensing methods for cognitive radio and the challenges associated with spectrum sensing is presented in [3]. In [4], a testbed to study dynamic spectrum access and analyze the coexistence between primary and secondary users was built. The authors used energy detection a threshold configured approximately 3 - 5 dB larger than the detected noise power. For that, they used a PC and a USRP (Universal Software Radio Peripheral) board with a software tool developed in C++. Similar work has been done in [5] where a statistical model for spectrum occupancy was proposed and implemented using USRP. A spectrum measurement setup and a model for duty cycle distribution were presented in [6]. Authors used a high-performance spectrum analyzer remotely controlled by a laptop via Ethernet. They deployed a Virtual Instrument Software Architecture (VISA) library with a MATLAB software for data gathering and analysis and applied energy detection

on a frequency range from 20MHz up to 6GHz. Authors in [7] studied the spectrum utilization pattern during a 24-hour period in Singapore in the frequency bands from 80 MHz to 5850 MHz. A survey was conducted for 12 weekday periods. They used Agilent spectrum analyzer connected to a computer by GPIB and used LabVIEW 8.2 software for data acquisition using energy detection. In [8], the authors introduced measurement tools to help in the process of providing spectrum utilization characterization for coexistence testing of wireless medical devices in the ISM band. The tools were tested using vector signal analyzer (VSA), vector signal transceiver (VST) and USRP. Other spectrum survey related references were provided in the same paper.

Accurate characterization of a wireless communication environment sometimes requires conducting long-term surveys which usually produce a large amount of data i.e. power measurements due to the significant frequent sampling required for accurate characterization of the environment. This would require either using hardware with high capabilities in terms of memory for data storage and retrieval and in terms of processors for data analysis; or reducing the data volume to get compact, accurate, and meaningful information out of it [2]. The former has been the focus of most of the methods proposed in the literature. For example, HDF5 data format standard was used for data storage in [9] where an RF observatory was built in Illinois, USA using USRP sensors and signal analyzers. The project generated terabytes of data in three years and a half. In [10] an improved storage system using a PostgreSQL database and Hadoop system was evaluated. A storage methodology called Tiered Storage of Generic Spectral Data (TSGSD) was introduced in [11] for long-term spectrum surveys used in observatories

in Chicago and Blacksburg, USA and in Turku, Finland. In [12] a supercomputer was used to store and process 6.5 TB of data generated by an 84-day spectrum survey conducted in the Children's Hospital at the University of Oklahoma Medical Center in Oklahoma City, USA. The authors used the frequency-domain data collection software detailed in [8].

Performance analysis of IEEE 802.11 Standard

IEEE 802.11 network performance and throughput analysis have been extensively studied both theoretically and experimentally and reported in the literature. In [13] a throughput analysis study was presented and a measurement-based mathematical model of the relationship between SNR and the delay was reported. Throughput-SNR models were also validated for both UDP and TCP protocols and for different file size. Similar studies for 802.11g and 802.11b were also cited at the same paper.

Empirical and theoretical studies of 802.11n has been presented in the literature. In [14] the performance of 802.11n standard for both TCP and UDP protocol throughput measurements were studied and compared to the same measurements of 802.11g to show the gain of 802.11n over 802.11g with and without implementing channel bonding. A similar but more extensive study was presented in [15] where an empirical throughput comparison study among 802.11a/b/g/n standards in an indoor environment was performed. Signal strength inside the coverage area of the different WLAN variants, average bandwidth, and average throughput measurements were reported. A more specific study to the features provided in 802.11n was introduced in [16] where the authors studied the behavior and the impact of the different channel

bonding choices on the network's management and performance optimization and the impact of the co-channel and adjacent channel interference on the network performance.

The authors in [17] investigated a measurement-based study of the IEEE 802.11ac performance in an indoor environment. They studied the changing in the throughput as the distance between the transmitter and the receiver increases and they investigated the effect of interference on the achieved throughput. The measurement setup comprised of two Asus RT-AC66U wireless routers that support all the mandatory IEEE 802.11ac features such as channel bonding up to 80 MHz, 256QAM modulation, and beamforming. To generate UDP traffic, they used IPerf and to capture and analyze packets they used Wireshark. Throughput was measured with varying communication range, the saturation throughout was measured to be around 612 Mbps with packet error rate less than 1%. They only studied UDP traffic and they did not model the relationship between throughput and SNR and no delay analysis were performed. Similar study can be found in [18] where a comparison of the theoretical and practical performances of both 802.11n and 802.11ac was explored in an office environment. The effect of both distance and interference between different channels was characterized. In [19] the authors presented the throughput performance characterization of TCP variants implemented in Linux operating systems for the IEEE 802.11ac and IEEE 802.11n standards based on an experimental study. They compared the performance of the two protocols for single-hop and multi-hop scenarios. They used three wireless mesh points each is Air5760 router with Broadcom BCM4360 chipset and they used IPerf as a traffic generator. The results showed that 802.11ac performs much better than 802.11n in the single-hop test while it does not have an important advantage over 802.11n for

multi-hop scenarios. In [20] a quantification of the gain in the average throughput provided by 802.11ac compared to IEEE 802.11n in the presence of interference caused by other 802.11n sources in an indoor environment. The experiments are performed for both Line of Sight (LOS) and Non-Line of Sight (NLOS) conditions using UDP traffic. All the experiments were repeated over a period of three days and the results were averaged. The results showed that 802.11ac provides higher average throughput than 802.11n operating in the 5GHz band and in both LOS and NLOS conditions. In [21] a theoretical study of 802.11ac wireless mesh backhaul network was presented. The authors assumed saturation conditions in the network and evaluated the MAC features of the protocol such as the downlink MU-MIMO, frame aggregation, and channel bonding. They also studied the Explicit Compressed Feedback (ECFB) channel sounding technique and extended the MU-RTC/CTS to integrate ECFB. They showed the results of their analytical model in addition to the simulation results with different spatial stream allocation algorithms. The results showed the gain acquired by the new features in the protocol and pointed out the scenarios where the protocol would give the highest gain. Another theoretical study was presented in [22] where the authors studied the performance of Dynamic Channel Access and Dynamic Bandwidth Operation features of 802.11ac using ns-3 simulator. The results showed the improvement in the throughput over the baseline 802.11ac with Static Channel Access scheme.

Chapter 3 – Software Development for Long-Term Surveys

PESA Implementation

Methodology

The focus of this chapter is to study the activity in the ISM unlicensed bands which are shared by technologies that have bursty wireless transmissions. PESA algorithm was proposed based on this characteristic of the activity on the wireless channel (i.e. busy periods followed by idle periods) [1]. While observing the wireless medium, it is noticed that the received power at the monitoring device is relatively constant during frames transmissions by a single transmitter and the transmit power is inversely proportional to the separation distance between the transmitter and the monitoring device. In PESA algorithm, the dynamic range of the monitoring device is divided into bins and represented by a mixture of Gaussian distributions proposed by Dr. Al-Kalaa with US FDA and given by Eq. (1). The mean and standard deviation of the noise component are estimated separately using a distribution fitter tool based on the actual observed noise power samples obtained from the intended environment.

$$G = \frac{1}{M+1}\left[\sum_{i=0}^{M-1} N\left(a + i * s, s\right) + N(\mu_N, \sigma_N)\right] \quad \text{Eq. (1)}$$

Where $N(\mu, \sigma) = N(x|\,\mu, \sigma) = \frac{1}{\sigma\sqrt{2\pi}} e^{-\frac{1}{2}\left(\frac{x-\mu}{\sigma}\right)^2}$; s is the bin width; μ_N, σ_N are the mean and the standard deviation of the noise, respectively; and M is the number of the GMM bins not including the noise bin.

The implementation of the PESA algorithm was developed in LabVIEW based on the time-domain data collection software developed by [8]. The basic software performs multiple functions such as acquiring I/Q data at a pre-specified I/Q sampling rate, processing it to obtain the power measurements, and finding duty cycle by

comparing with a threshold. In parallel, the raw power measurements are inserted into PESA real-time processing queue where windows of activity/inactivity regions are defined based on a fixed activity decision threshold T which was chosen to exceed the detected noise mean by 3-5 dB based on [23]. A smoothing filter was used to solve the problem of having outliers in the measurements i.e. fluctuations of the power measurements. All the consecutive power measurements that exceed T are considered an activity. After that, the average values of the activity windows are calculated and compared with the means of the GMM components (bins) to find the component with the largest posterior probability for the observed averages. In other words, a window average is assigned to a bin index if the average belongs to $[\mu - s/2\,, \mu + s/2\,]$where s is the bin width. The inactivity windows are assigned to the dedicated noise component. Finally, the indices of the responsible GMM components and the length of the activity/inactivity windows are saved into a text document. The PESA system processing flow for the intended environment is depicted in Figure 1. and the LabVIEW implementation is detailed in Algorithm 1.

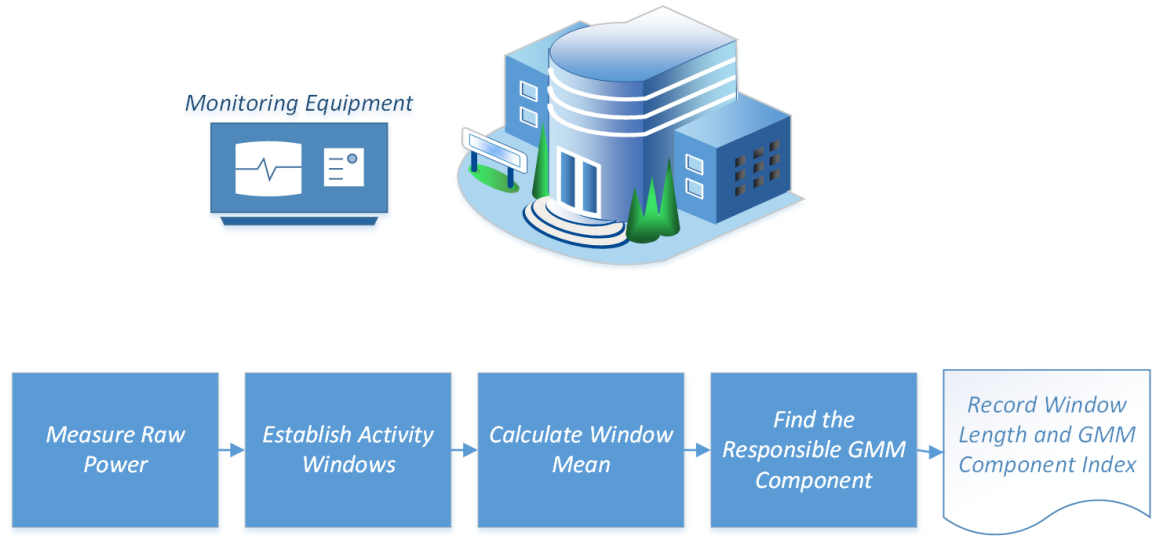

Figure 1. PESA System Processing Flow.

Algorithm 1 LabVIEW Implementation

Input : $DR_{min}, DR_{max}, Bin\ Size, Threshold$
Output: *Length, Component's Index*
$(\mu_N, \sigma_N) \leftarrow$ *Noise Mean and Standard Deviation*
$Threshold \leftarrow \mu_N + x\ dB$
Calculate the number of components (M):
if $mod(\frac{DR_{max}-DR_{min}}{Bin\ Size}) = 0$ **then**
    $M \leftarrow \lceil \frac{DR_{max}-DR_{min}}{Bin\ Size} \rceil + 1$
else
    $M \leftarrow \lceil \frac{DR_{max}-DR_{min}}{Bin\ Size} \rceil$
end if
for $i \leq M$ **do**
    $GMM_means \leftarrow [DR_{min} + (i \times Bin\ Size)]$
end for
while Processing Queue is not empty **do**
    $F = f_1, f_2, ..., f_m$
    $W = w_1, w_2, ..., w_m$: where w_j is the jth group of elements from F who are either continuously greater than the threshold or less than or equal the threshold.
end while
for *all w in W* **do**
    $Length \leftarrow Length(w)$
    $X \leftarrow E(w)$
end for
for *all x in X* **do**
    if x is the average of an active window **then**
        if $[GMM_means(i) - \frac{Bin\ Size}{2}] \leq x < [GMM_means(i) + \frac{Bin\ Size}{2}]$ **then**
            $Component's\ Index \leftarrow i$
        end if
    else
        $Component's\ Index \leftarrow 1$
    end if
end for
Return Length, Component's Index

Hardware

The hardware that was used in the development process is a VST built on an NI PXIe platform. The VST is a new generation of instrumentation that combines a VSA and a VSG (Vector Signal Generator) with FPGA-based real-time signal processing and control which permits a significant reduction in the RF measurement processing time. However, the flexibility and the generality of the developed software make it easy to be ported to other platforms with no required change in the processing methodology. The developed software could work on either VST or VSA without changing or adding to the input parameters. Moreover, porting the software to the USRP platform is also possible after taking into consideration any changes in the aggregated gain and offset applied to the RF signal. The developed software can be broadly applied to any platform and easily adjusted to meet the requirements of the environment and the available resources.

Experimental Results

To validate the LabVIEW implementation objectives, a spectrum survey was conducted at the University of Oklahoma Family Medicine Center in Tulsa, OK, USA. The surveyed location is a clinic that has 3 floors with around 43 primary and specialty healthcare providers.

The hardware used consisted of NI PXIe-5644R [24] with NI PXIe-8135 embedded controller [25]. The VST has an average noise level of 157 dBm/Hz, 80 dB spurious-free dynamic range, and 50 MHz instantaneous bandwidth (at 3 dB). The test equipment was installed in a hallway in the healthcare center, with the distance between the antenna of ME and the closest WiFi AP is 1.5 meters diagonal while other APs in the surveyed environment were active at further distances.

To determine the activity threshold, a noise estimation process was performed to determine the noise mean in the environment. A pre-test was conducted in the environment and the raw power data were fitted into a normal distribution using MATLAB's built-in distribution fitter tool. The activity threshold was set to 8 dB above the noise mean to minimize the false detection error. For the surveyed environment, the activity threshold was fixed at -74.6 dBm throughout the survey. WLAN channel 1 centered on 2412 MHz was monitored during the survey with an I/Q sampling rate fixed at 1 MS/s and a smoothing filter of length 3 to minimize the fluctuations in the measurements.

The survey lasted 7 hours, on Dec. 1st, 2017 commencing at 10:16 AM and ending at 5:16 PM. Both the original power measurements and PESA output were stored on a hard drive for validation and comparison purposes. The original

measurements file sizes ware approximately 8.4 GB while PESA output required only 96.28 MB storage volume which decreased the storage volume by approximately 98.8%. Figure 2. illustrates a comparison in the storage volume for the original and the regenerated measurements.

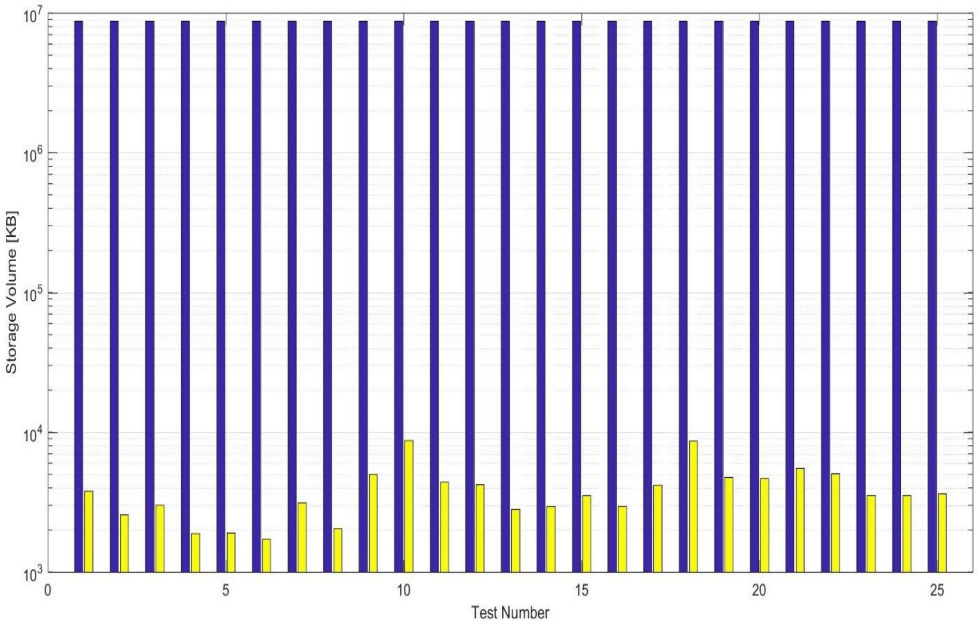

Figure 2. Comparison of the storage volume between the original power samples and the PESA output CSV files. The data generated from the survey was saved into 25 16-minute long separate files.

Channel Utilization was used as a metric to evaluate the results of PESA algorithm. Channel utilization represents the percentage of time during which a channel is occupied. PESA output was used to generate the power measurements based on the stored GMM indices and then used to calculate the channel utilization with 1-s time resolution. Figure 3. depicts a comparison between a sample of the original power measurements and the regenerated ones using PESA output. The results show that the power samples generated using PESA output closely match the original power samples. Channel utilization variations during the survey period were fitted into a Generalized

Extreme Value distribution [12] as shown in Figure 4. The channel utilization values remain close to a minimum value with a mean of 1.1% and a standard deviation of 0.38%. However, there were some higher activity occurrences throughout the survey period with a maximum value of 53.8%. Moreover, the estimation error was evaluated, and the error mean for all the calculated values of channel utilization was 1.19%. Eq. (2) was used to calculate the error.

$$\text{Error_CU} = Mean\ (100 * \ |CU_orig - CU_regen|/CU_orig) \quad \text{Eq. (2)}$$

Where CU_orig is the channel utilization calculated using the original observed power values and CU_regen is the channel utilization calculated using the power values generated using PESA output.

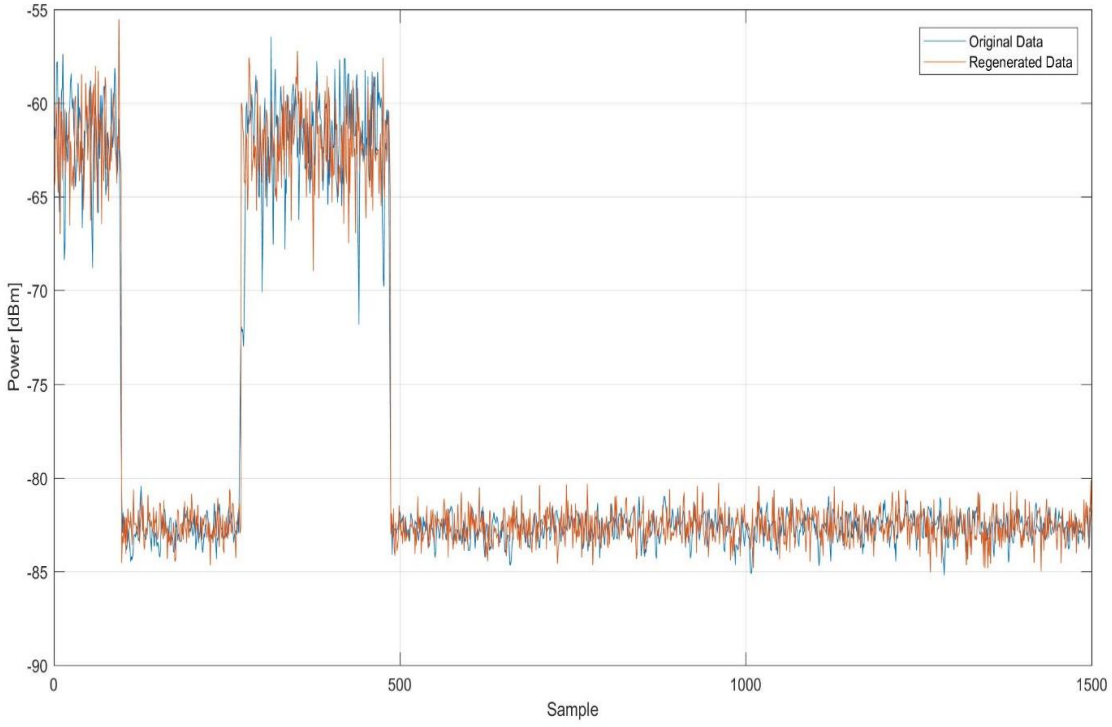

Figure 3. Comparison between the original power measurements and the regenerated ones using PESA.

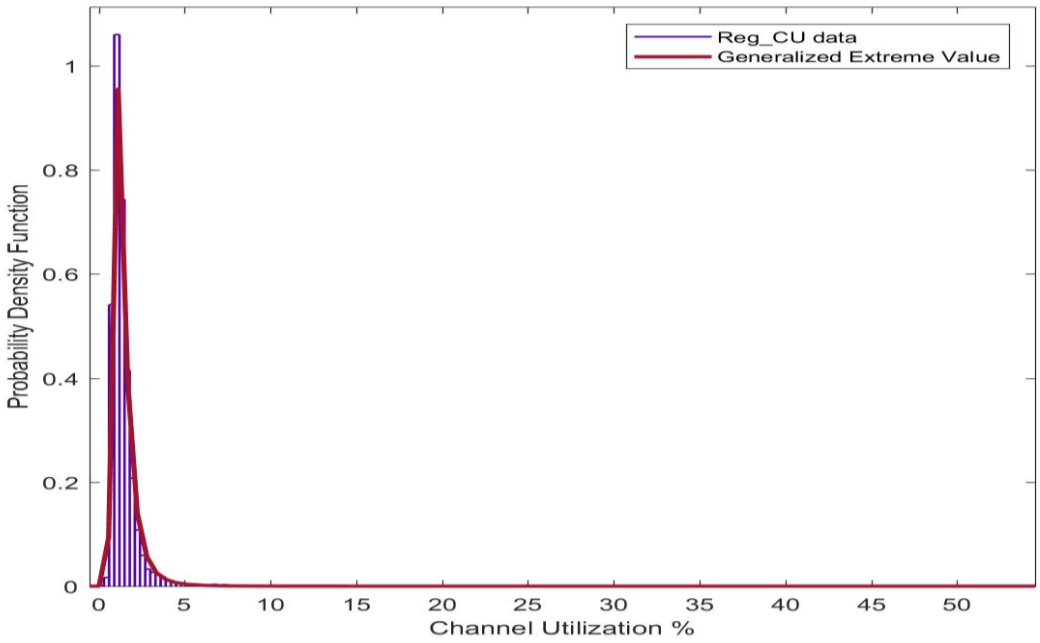

Figure 4. The fitted PDF of the Channel Utilization calculated using PESA output.

Discussion

The results of the real-time implementation of PESA algorithm proposed by Dr. Alkalaa with US FDA were reported in the previous section. The results of the 7-hour survey demonstrate that the probabilistic efficient storage algorithm maintains an accurate estimation of channel utilization as the estimation error was on average 1.19%. Furthermore, it preserves the temporal characteristics of the spectrum occupancy, while reducing the storage volume required to save a large number of samples needed for an accurate and high-quality channel utilization. The reduction achieved for the data generated during the survey was 98.85%. This algorithm could facilitate conducting spectrum surveys which are very significant for the study of wireless coexistence and spectrum sharing.

The implementation of the proposed algorithm with has the following limitations:

1. An accurate estimation of the noise level should be performed separately prior to using the software.
2. The channel utilization estimation using the algorithm is highly affected by the variation in the power level which makes it more suitable for a 1-AP network, in the case of using a fixed activity threshold.

Chapter 4 – IEEE 802.11ac Performance Analysis

IEEE 802.11ac Standard

WLAN systems started with using 802.11b, 802.11g, and 802.11a standards, which provided throughput enhancements over the original 802.11 PHY. And the progress continued with the development of 802.11n with introducing frame aggregation, channel bonding, higher MCS, and multiple-input multiple-output (MIMO). IEEE 802.11ac is one of the 802.11 wireless networks' standards family which was published in 2013 and was developed to provide very high throughput (VHT) wireless local area networks (WLANs) in the 5 GHz unlicensed band. A comparison among the theoretical throughput of different 802.11 standards is shown in Figure 5. where 802.11ac offers the highest throughput when using MIMO with 4 spatial streams and 80 MHz channel bandwidth compared to 802.11n with 40 MHz channel bandwidth.

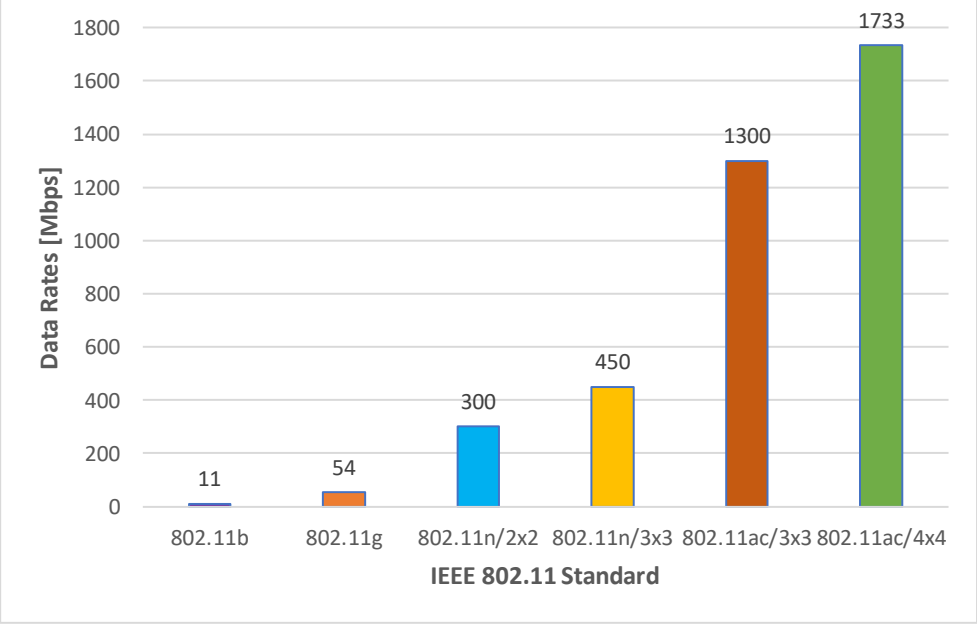

Figure 5. IEEE 802.11 Maximum Theoretical Data Rates.

PHY and MAC Layer Enhancements

IEEE 802.11ac, on one hand, maintains most of the PHY features of 802.11n such as the use of binary convolutional coding (BCC) for forward error correction, the basic MIMO, and the modulation and coding schemes (MCSs) 0 to 7. On the other hand, the standard extends some of the PHY features of 802.11n. For example, the support of 80 MHz and 160 MHz channel bandwidth as compared to 802.11n where 40 MHz is the largest channel bandwidth, with the possibility of using non-contiguous 80 MHz channels to form a 160 MHz channel. Figure 6. shows the channelization for 802.11ac standard [27], Figure 7a. demonstrates the channel-list elements for 40 MHz, 80 MHz, and160 MHz channel width, while Figure 7.b illustrates the channel-list elements for 80+80 MHz channel width [28].

Furthermore, 802.11ac supports two new MCSs 8 and 9 that are based on 256-QAM modulation with code rates of 3/4 and 5/6; and it extends the possible number of spatial streams up to 8 as compared to a maximum of 4 spatial streams in 802.11n.

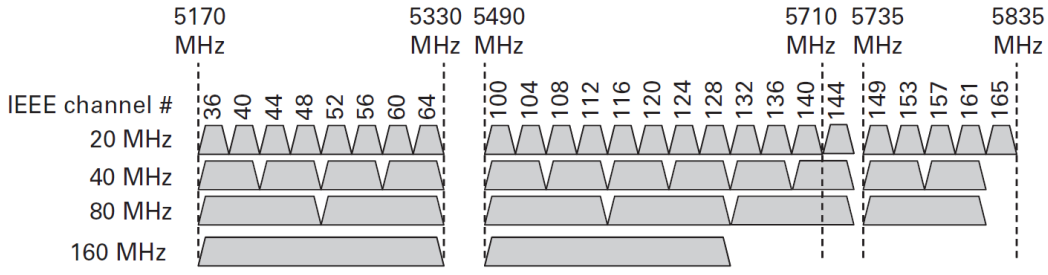

Figure 6. The channelization in the IEEE 802.11ac standard.

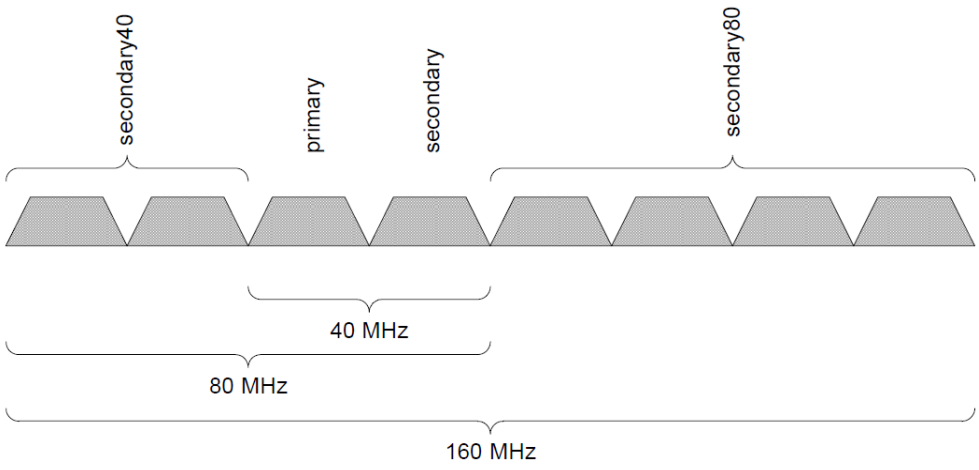

(a)

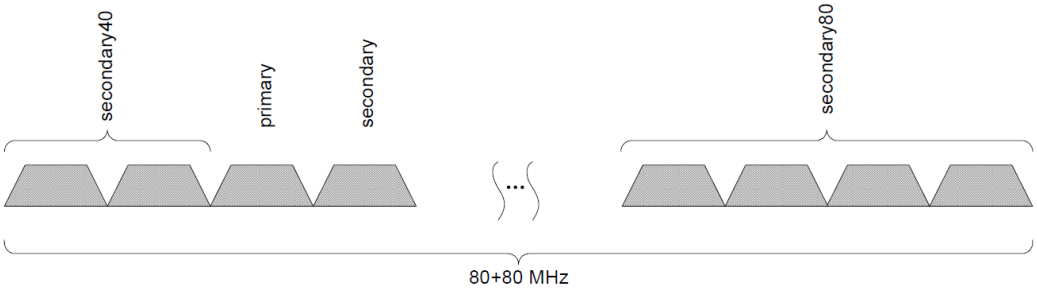

(b)

Figure 7. The channel-list elements for 802.11ac. a) 40 MHz, 80 MHz, and 160 MHz channel width. b) 80+80 MHz channel width.

Similar to the PHY features enhancements introduced in 802.11ac, the protocol preserves and further extends the MAC features of the 802.11n protocol. The 802.11ac maintains the frame aggregation and block acknowledgment features introduced in 802.11n but supports enhanced A-MSDU and A-MPDU in which the maximum MPDU size and the PSDU length are increased to 11426 bytes and to 4692480 bytes, respectively with no direct constraint on the maximum A-MSDU size [28]. Moreover, since 802.11ac is a VHT protocol, it introduces VHT capabilities such as Multi-User MIMO (MU-MIMO), Transmit Beamforming (TxBF) with compressed feedback, and

fast link adaptation. Figure 8. and Figure 9. Demonstrate the PHY frame format and the MAC frame format, respectively [28].

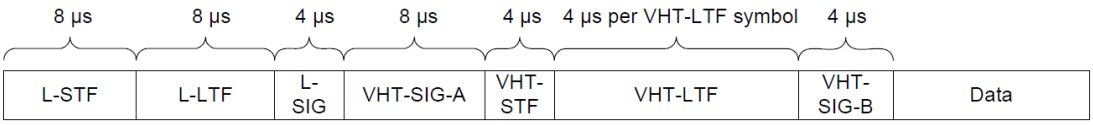

Figure 8. VHT PPDU Format.

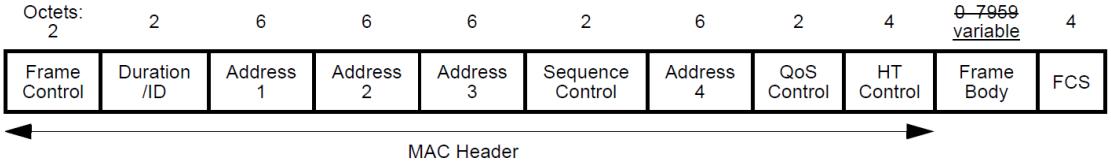

Figure 9. MAC Frame Format.

Experimental Setup

The test setup depicted in Figure 10. consisted of one-pair 802.11ac network. The nodes were Mikrotik router boards 953GS-5HnT-RP [29] with R11e-5HacD wireless card [30] which supports 256-QAM modulation, two spatial streams, and channel bonding up to 80 MHz channel bandwidth. The router boards can be configured to function as IEEE 802.11 standards that operates in the 5 GHz band. The router boards run a networking embedded operating system called "RouterOS" which offers a graphical interface allowing the user to change the board's configuration as well as a set of performance analysis tools such as bandwidth test and ping.



Figure 10. IEEE 802.11ac Measurement Setup.

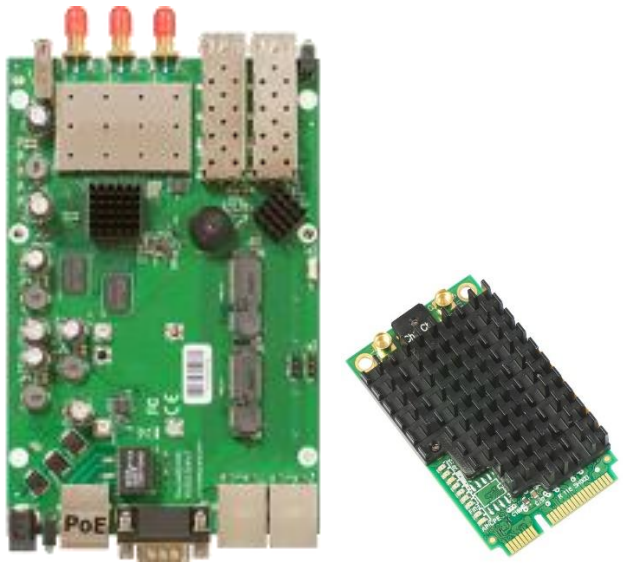

Figure 11. Mikrotik router boards 953GS-5HnT-RP with R11e-5HacD wireless card.

One node was configured to operate as an access point (transmitter) and the other as a station (receiver), and the router boards were configured to use their maximum operational power during all the tests and it was fixed at 16 dBm. The performance analysis tools offered by the boards were used to develop the empirical model in this thesis.

The experiments were conducted in an underground laboratory room with low noise floor (< -95 dBm) to ensure that no other wireless activity in the 5 GHz band during the tests exist and develop accurate models. The throughput analysis was performed separately from the delay analysis, and the SNR at the receiving node was varied by changing the spatial distribution of the nodes, by changing the distance between the AP and the STA.

Experimental Results

Throughput Analysis without the Interference

Traffic was generated using the bandwidth test tool provided by the RouterOS operating system. Both User Datagram Protocol (UDP) and Transmission Control Protocol (TCP) protocols were evaluated. UDP is a connectionless protocol as it does not require establishing a virtual circuit before data transfer begins, unlike TCP which provides a reliable data exchange and error control through acknowledgments.

The boards were set to operate on the center frequency of 5220 MHz with two spatial streams and channel bandwidth of 20 MHz, 40 MHz, and 80 MHz to demonstrate the effect of channel bonding on the throughput. Each test was repeated 5 times and an average was calculated.

Figure 12. illustrates a comparison among the network throughput of the three channel bandwidths. The graph shows the advantage of the channel bonding feature available in the 802.11ac standard where the throughput increases as the channel bandwidth increases.

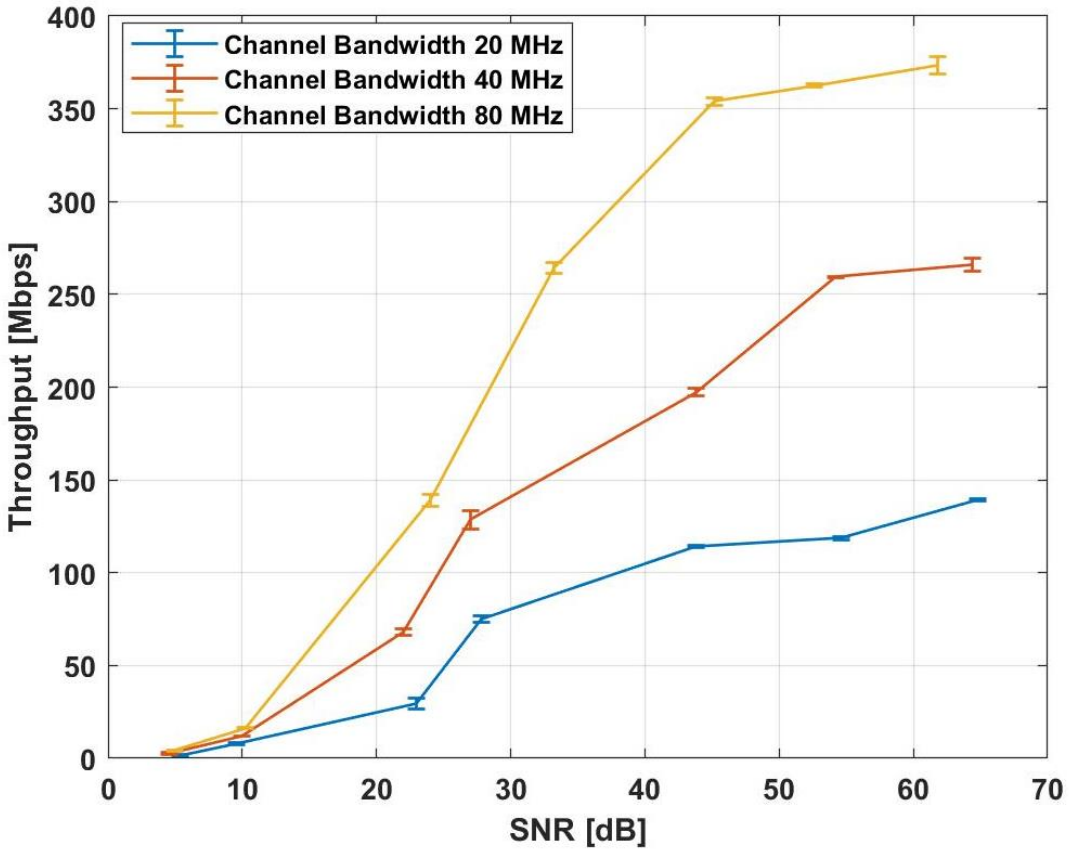

Figure 12. Comparison of throughput vs SNR for different channel bandwidths for UDP Protocol and two spatial streams.

The throughput measurements for varied channel bandwidth was then mathematically modeled using smoothing cubic spline interpolation.

Cubic spline interpolation is a piecewise-polynomial approximation where a cubic polynomial given by (3) is used on the subintervals between two consecutive data points where this polynomial has continuous first and second derivative on the overall interval [31].

$$S_i(x) = a_i + b_i(x - x_i) + c_i(x - x_i)^2 + d_i(x - x_i)^3 \qquad (3)$$

Where $i = 0, 1, \ldots\ldots, n\text{-}1$ and $S_i(x)$ is a cubic polynomial on the subinterval $[x_i, x_{i+1}]$. The parameters a_i, b_i, c_i, and d_i are calculated so they satisfy the following conditions:

(a) $S_j(x_j) = f(x_j)$ and $S_j(x_{j+1}) = f(x_{j+1})$ for each $j = 0, 1, \ldots, n-1$;

(b) $S_{j+1}(x_{j+1}) = S_j(x_{j+1})$ for each $j = 0, 1, \ldots, n-2$;

(c) $S'_{j+1}(x_{j+1}) = S'_j(x_{j+1})$ for each $j = 0, 1, \ldots, n-2$;

(d) $S''_{j+1}(x_{j+1}) = S''_j(x_{j+1})$ for each $j = 0, 1, \ldots, n-2$;

Smoothing cubic spline is a cubic spline with a polynomial that minimizes the function given in Eq. (4) [32].

$$RSS\ (S,p) = \ p\sum_{i=1}^{n}[f(x_i) - S(x_i)]^2 + (1-p)\int\left(\frac{d^2S}{dx^2}\right)^2 dx \quad \text{Eq. (4)}$$

Where p is the smoothing parameter and takes values between [0,1].

The throughput models for UDP protocol are shown in Figure 13. and the smoothing parameter values, as well as the goodness-of-fit statistics for the throughput model for the three channel bandwidths, are given in Table [1]. SSE is the sum of squared errors or the sum of the squares of residuals i.e. the deviations of the approximated values from the empirical values of data and is given in Eq. (5).

$$SSE = \sum_{i=1}^{n}[f(x_i) - S(x_i)]^2 \quad \text{Eq. (5)}$$

RMSE is the root mean squared error which represents the standard deviation of the differences between the approximated values and the empirical values of data and given by Eq. (6).

$$RMSE = \sqrt{\frac{\sum_{i=1}^{n}[f(x_i)-S(x_i)]^2}{n}} \quad \text{Eq. (6)}$$

And R-squared is the coefficient of determination which represents the correlation between the approximated values and the empirical values of data and given by Eq. (7).

$$R - squared = 1 - \frac{SSE}{SST} \quad \text{Eq. (7)}$$

Table 1. Statistics of the IEEE 802.11ac throughput model for UDP Protocol.

	20 MHz	40 MHz	80 MHz
p	0.35	0.61	0.55
SSE	0.0764	0.2041	0.07439
RMSE	1.223	2.116	1.372
R-squared	0.9996	0.9997	0.9999

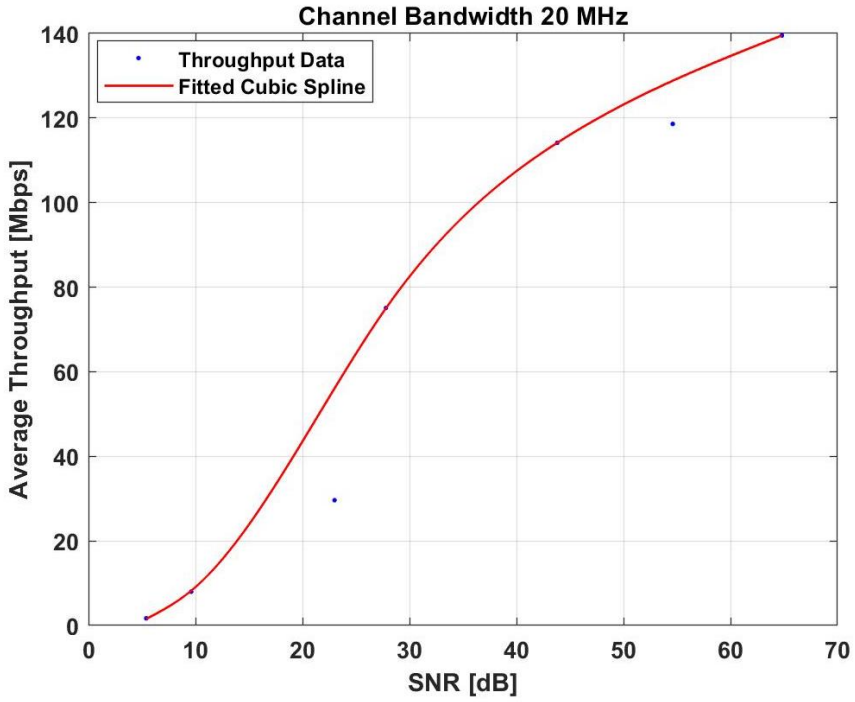

(a)

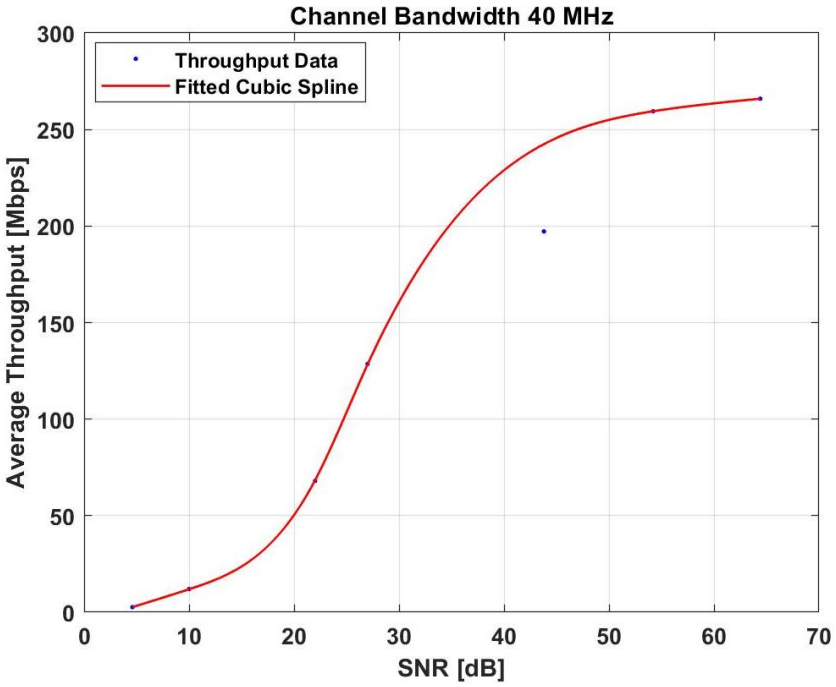

(b)

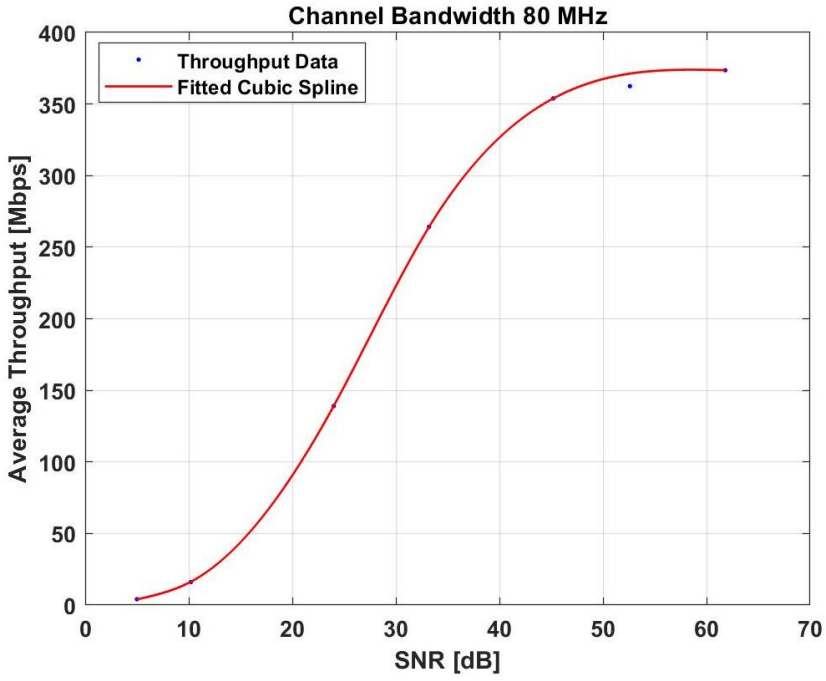

(c)

Figure 13. IEEE 802.11ac throughput vs SNR model for UDP Protocol and two spatial streams. a) 20 MHz channel width. b) 40 MHz channel width. c) 80 MHz channel width.

Another approach to mathematically model the network capacity in terms of SNR is based on Shannon's theorem. It sets the upper limit on the capacity whose formula is given by Eq. (8).

$$C = a * N_{ss} * B * log_2(1 + SNR) + b \qquad \text{Eq. (8)}$$

Where C is the maximum capacity (bits/s), B is the channel bandwidth, SNR is the signal-to-noise ratio, and N_{ss} is the number of spatial streams [33].

Capacity formula is given by Eq. (8) where the parameter a represents the effect of N_{ss} on the throughput for different channel width options, and b represents the decrease in the throughput related to the overhead added at each OSI layer up to the transport layer. The parameters a and b were estimated and are shown in Table [2] with 95% confidence intervals. Table [3] presents the goodness-of-fit parameters for the logarithmic model. Moreover, Figure 14 shows the UDP throughput model for different channel bandwidths based on Eq. (8) and using N_{ss} of 2 to match the experimental setup.

Table 2. Coefficients of the logarithmic model of the IEEE 802.11ac throughput.

	a	95% confidence Interval	b	95% confidence Interval
20 MHz	2.15e-06	[1.335e-06, 2.966e-06]	-132.2	[-211.1, -53.41]
40 MHz	4.057e-06	[2.48e-06, 5.634e-06]	-244.2	[-395.8, -92.7]
80 MHz	6.22e-06	[4.235e-06, 8.205e-06]	-371.3	[-564.4, -178.2]

Table 3. Statistics of the logarithmic model of the IEEE 802.11ac throughput.

	20 MHz	40 MHz	80 MHz
SSE	1895.5	7554.6	11333
RMSE	19.4704	38.8706	47.6097
R-squared	0.9018	0.8974	0.9285

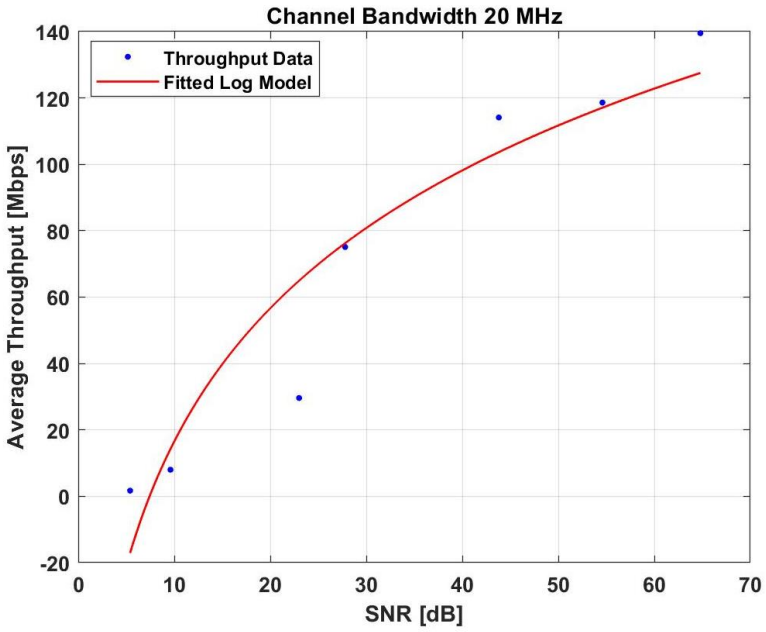
Channel Bandwidth 20 MHz
Throughput Data
Fitted Log Model
Average Throughput [Mbps]
SNR [dB]
140
120
100
80
60
40
20
0
-20
0
10
20
30
40
50
60
70

(a)

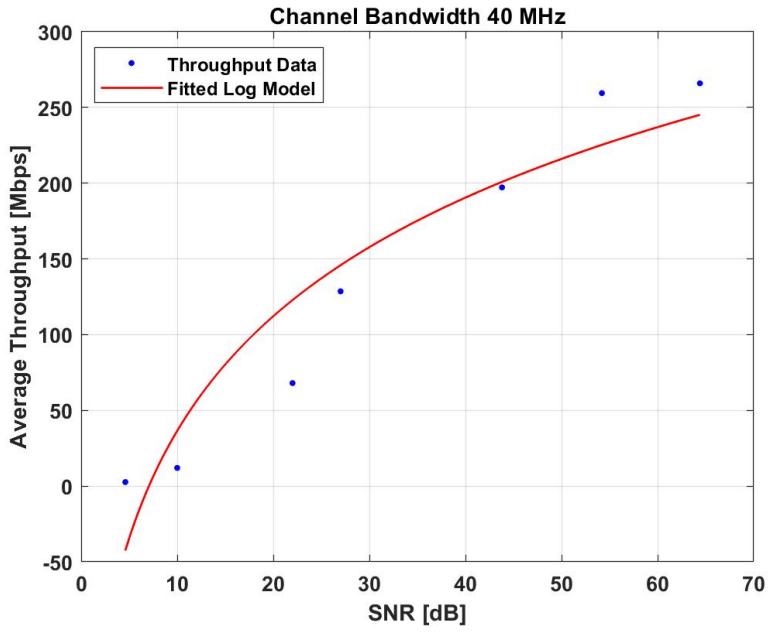
Channel Bandwidth 40 MHz
Throughput Data
Fitted Log Model
Average Throughput [Mbps]
SNR [dB]
300
250
200
150
100
50
0
-50
0
10
20
30
40
50
60
70

(b)

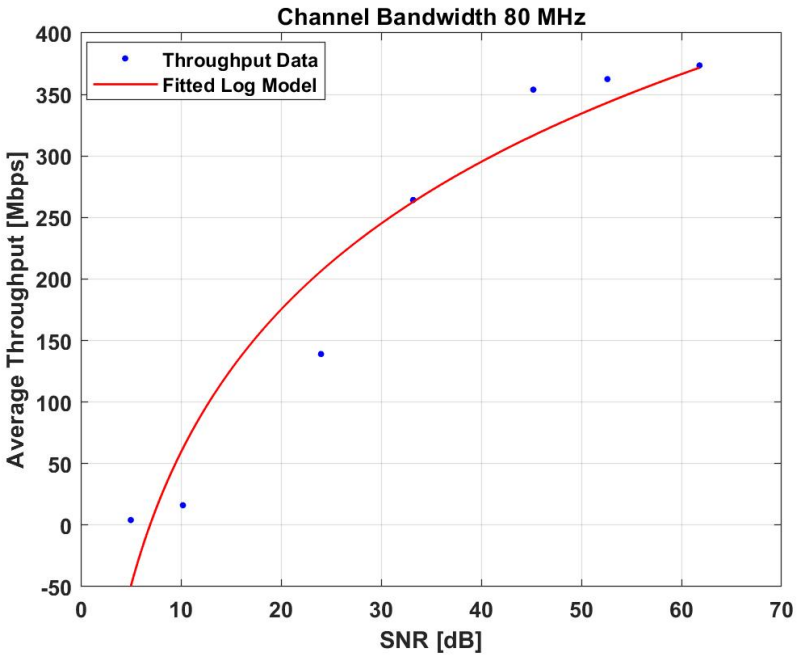

(c)

Figure 14. IEEE 802.11ac throughput vs SNR logarithmic model for UDP Protocol and two spatial streams. a) 20 MHz channel width. b) 40 MHz channel width. c) 80 MHz channel width.

The TCP throughput measurements were also fitted into mathematical models using smoothing cubic spline interpolation. Figure 15. depicts a comparison among the network throughput of the three channel bandwidths for TCP protocol and the throughput models are shown in Figure 16. while the smoothing parameter values and the goodness-of-fit statistics for the throughput model for the three channel bandwidths are given in Table [4].

Table 4. Statistics of the IEEE 802.11ac throughput model for TCP Protocol.

	20 MHz	40 MHz	80 MHz
p	0.51	0.18	0.38
SSE	0.4874	0.7953	0.6932
RMSE	0.9297	0.8225	1.8024
R-squared	0.9994	0.9998	0.9992

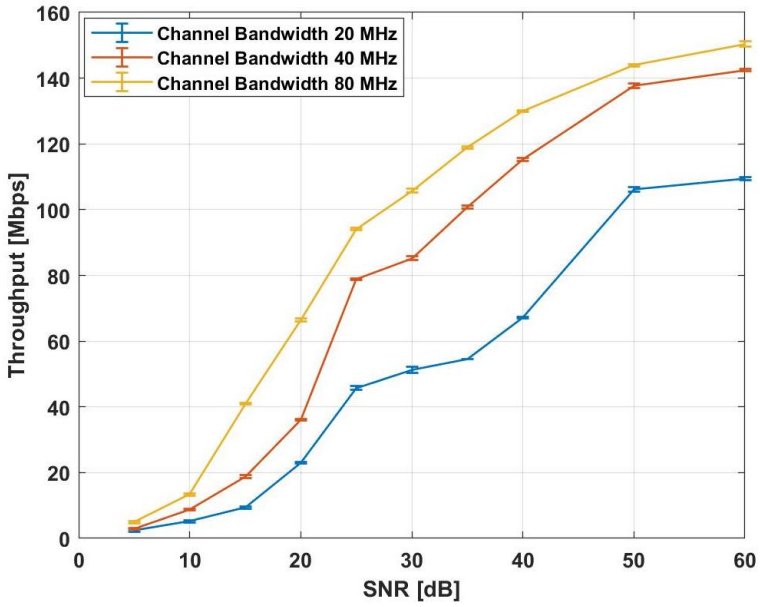

Figure 15. Comparison of throughput vs SNR for different channel bandwidths for TCP Protocol and two spatial streams.

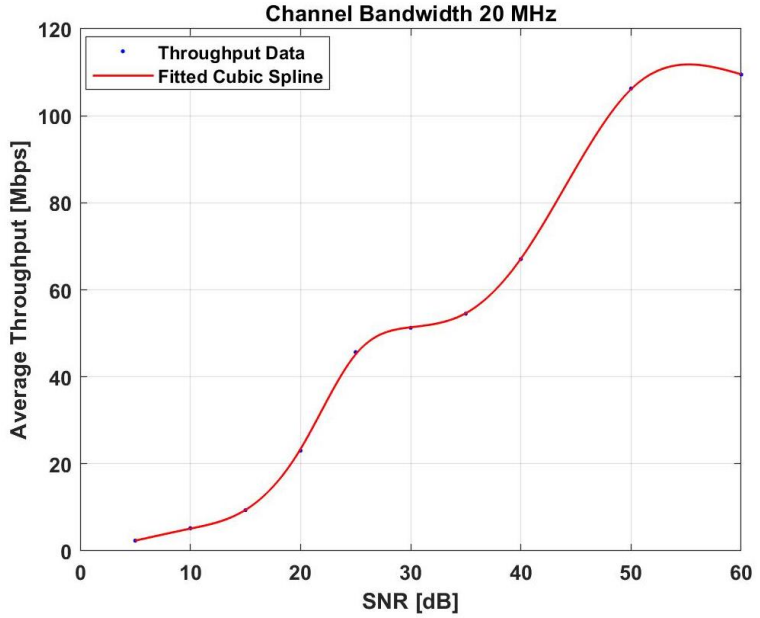

(a)

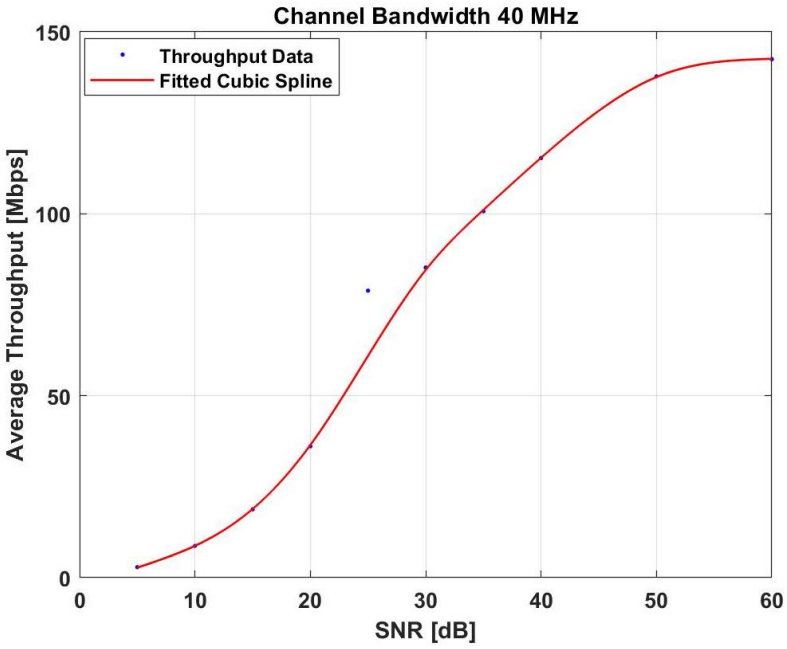

(b)

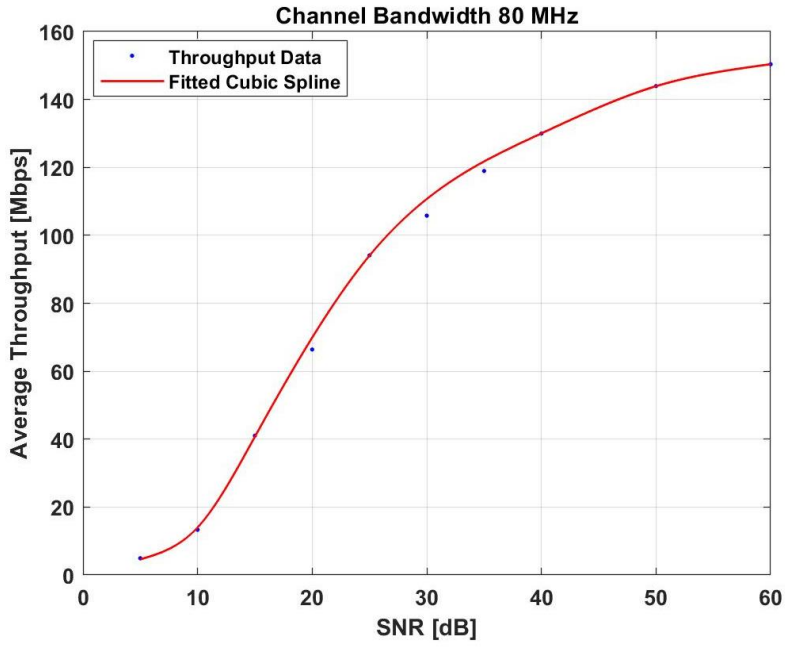

(c)

Figure 16. IEEE 802.11ac throughput vs SNR model for TCP Protocol and two spatial streams. a) 20 MHz channel width. b) 40 MHz channel width. c) 80 MHz channel width.

The effect of the number of used spatial streams was evaluated experimentally. A test was conducted for an IEEE 802.11ac network running on the center frequency of 5220 MHz with channel bandwidth of 80 MHz and one spatial stream. Both UDP and TCP protocols were studied. Figure 17.a demonstrates a comparison between the network throughput for UDP and TCP protocols when one spatial stream was used. Figure 17.b shows the two spatial streams case. Moreover, Figure 18. depicts a comparison between the network throughput when using one spatial stream and two spatial streams for UDP Protocol.

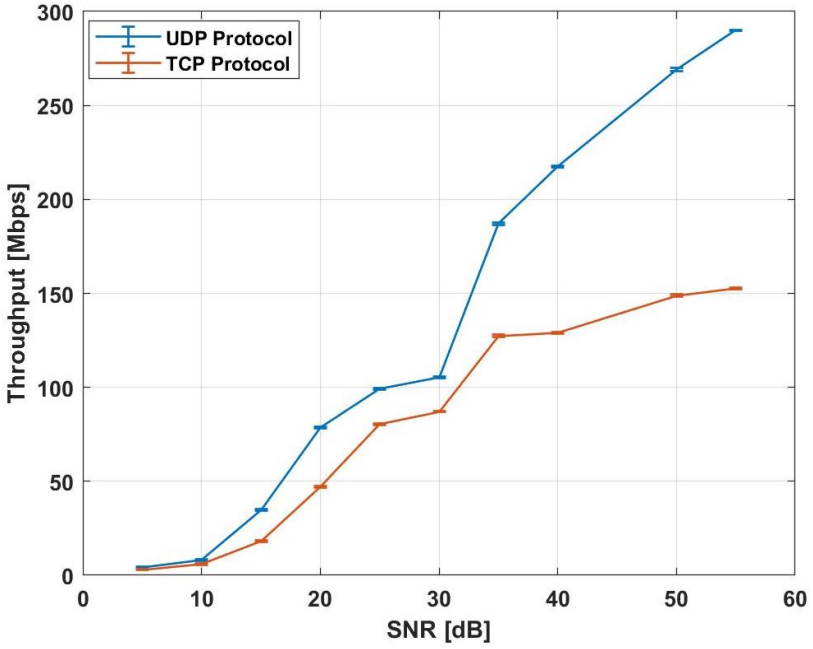

(a)

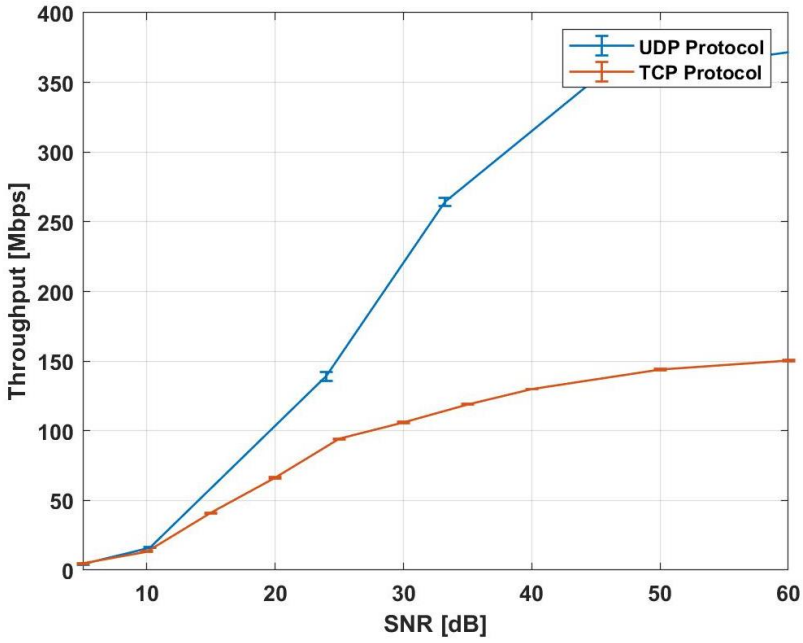

(b)

Figure 17. Comparison between the throughput of IEEE 802.11ac with 80MHz channel bandwidth for UDP and TCP Protocols a) One spatial stream. b) Two spatial streams.

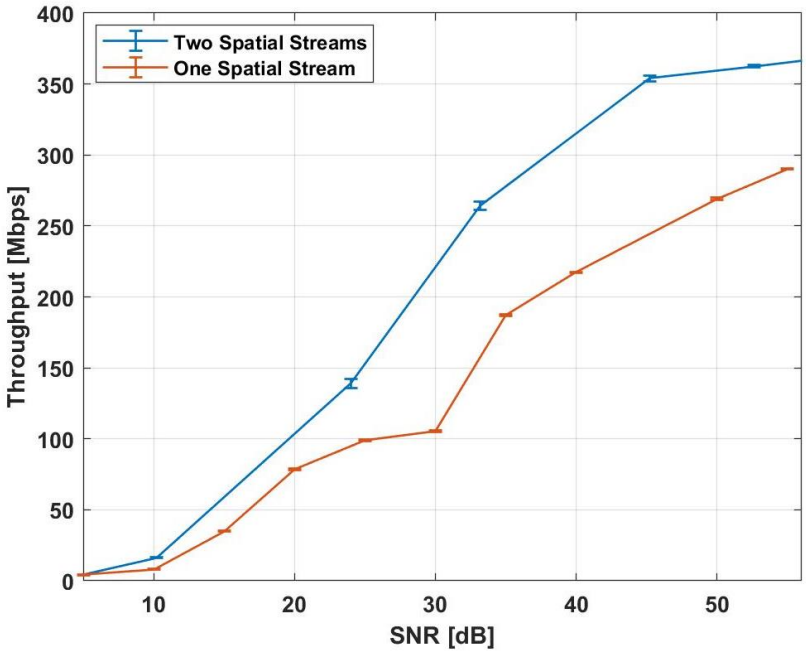

Figure 18. Comparison between the throughput of IEEE 802.11ac with 80MHz channel bandwidth when using one spatial stream and two spatial streams for UDP Protocol.

Throughput Analysis with the Interference

To generate interference, a similar IEEE 802.11ac nodes pair was used. Both the interfering pair and the main 802.11ac pair (DUT) were configured similarly. They were set to operate on the center frequency 5220 MHz with a channel bandwidth of 80 MHz and two spatial streams yielding the worst-case interference scenario. The test setup is depicted in Figure 19. where the distance between the DUT transmitter and receiver was fixed to 1 m while the distance between the interferer transmitter and receiver was changing to vary the value of the Signal to Interference Ratio (SIR) at the DUT receiving node.

Traffic was generated using the bandwidth test tool for UDP protocol and the throughput was measured for varied SIR values. The throughput measurements for the two networks is shown in Figure 20. where we can see that for low SIR values (<10 dB) the interfering network is dominating the channel by achieving a higher throughput and as SIR increases i.e. the distance between the interferer transmitter and receiver decreases, the throughput of the DUT network increases as a result to the drop in the interferer's throughput.

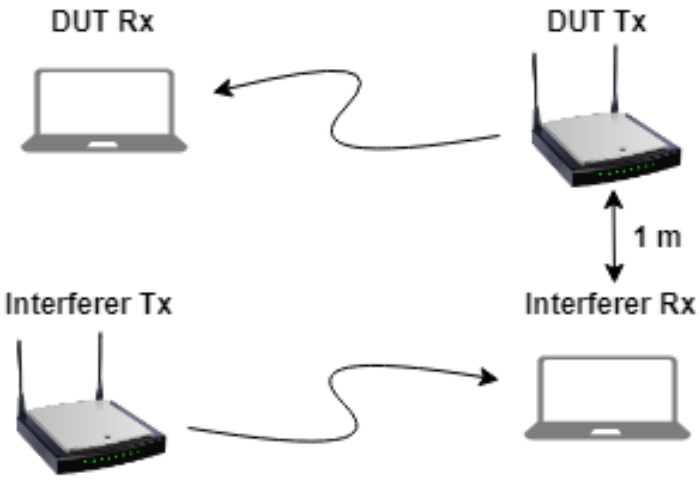

Figure 19. The measurement Setup in the presence of the interfering network.

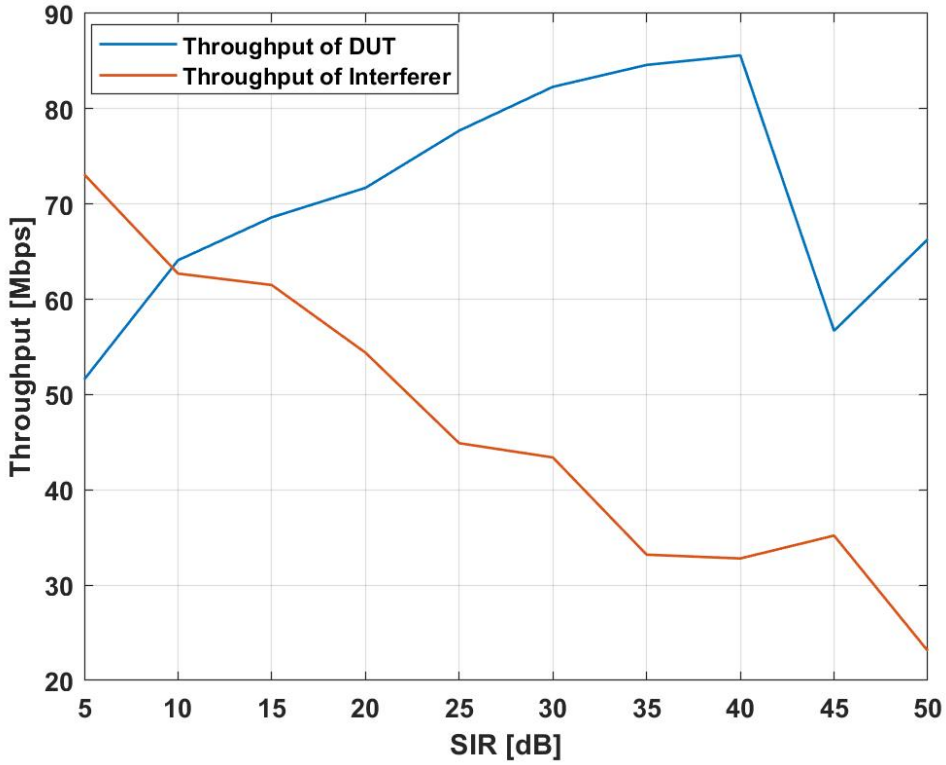

Figure 20. Comparison between the throughput of the IEEE 802.11ac DUT network and the Interfering network.

Delay Analysis

Internet Control Message Protocol (ICMP) Echo messages were used in the analysis and to determine the round-trip delay when communicating using the Ping tool. The AP sends ICMP message to the STA and waits for the ICMP echo-reply. The interval between these events is the round-trip time. In each test 1000 messages with a size of 1500 Bytes are exchanged between the AP and the STA and the average round-trip time is reported.

Figure 21. depicts a comparison among the network delay of the three channel bandwidths.

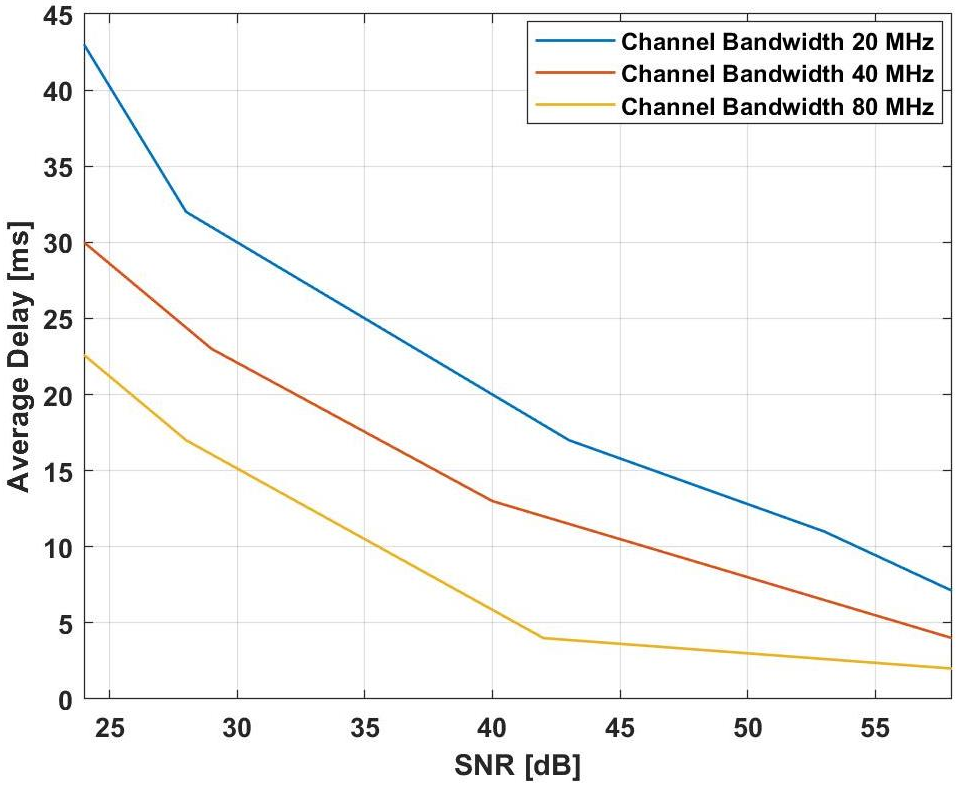

Figure 21. Comparison of Delay vs SNR for different channel bandwidths.

The delay measurements for varied channel bandwidth were mathematically modeled using exponential distribution given by Eq. (10).

$$f(x) = a * e^{bx} \qquad \text{Eq. (10)}$$

The delay models are shown in Figure 22. and the goodness-of-fit statistics for the delay model for the three channel bandwidths are given in Table [5] while Table [6] shows the coefficients of the exponential models with 95% confidence level.

Table 5. Statistics of the IEEE 802.11ac delay model.

	20 MHz	40 MHz	80 MHz
SSE	13.3402	1.9064	2.5909
RMSE	2.1087	0.7972	0.9293
R-squared	0.9868	0.9962	0.9934

Table 6. Coefficients of the IEEE 802.11ac delay model.

	a	95% confidence Interval	b	95% confidence Interval
20 MHz	141.9	[77.27, 206.6]	-0.05095	[-0.06663, -0.03528]
40 MHz	112.2	[82.98, 141.4]	-0.05473	[-0.06368, -0.04578]
80 MHz	158.6	[71.13, 246.1]	-0.08148	[-0.1029, -0.06007]

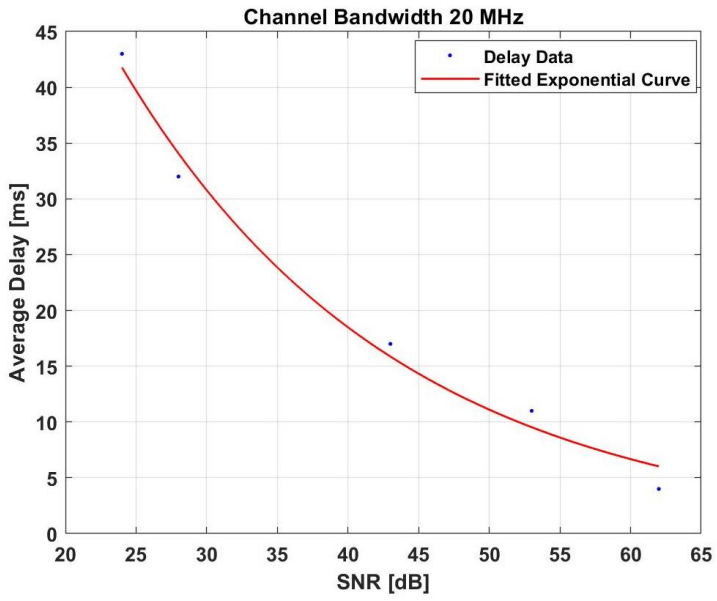

(a)

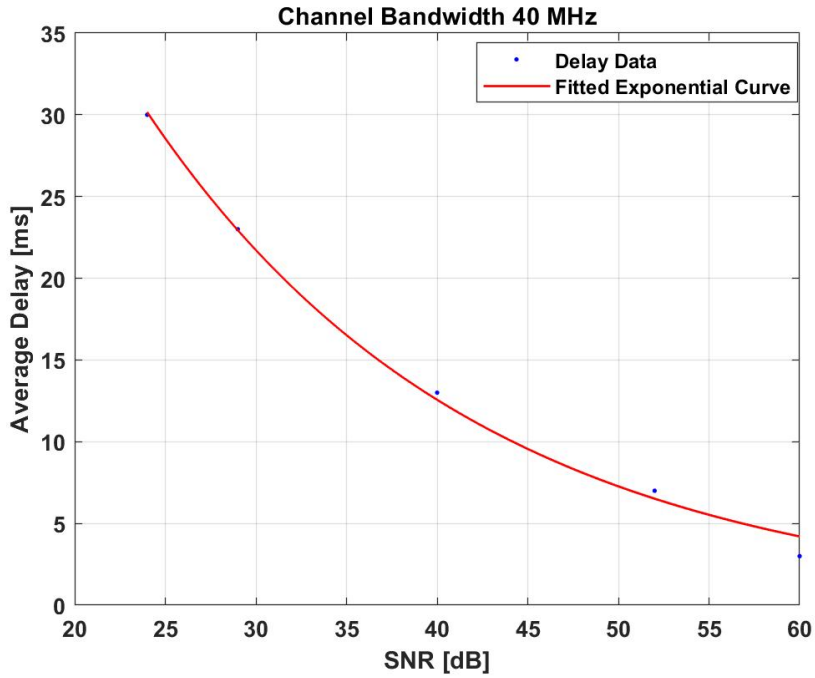

(b)

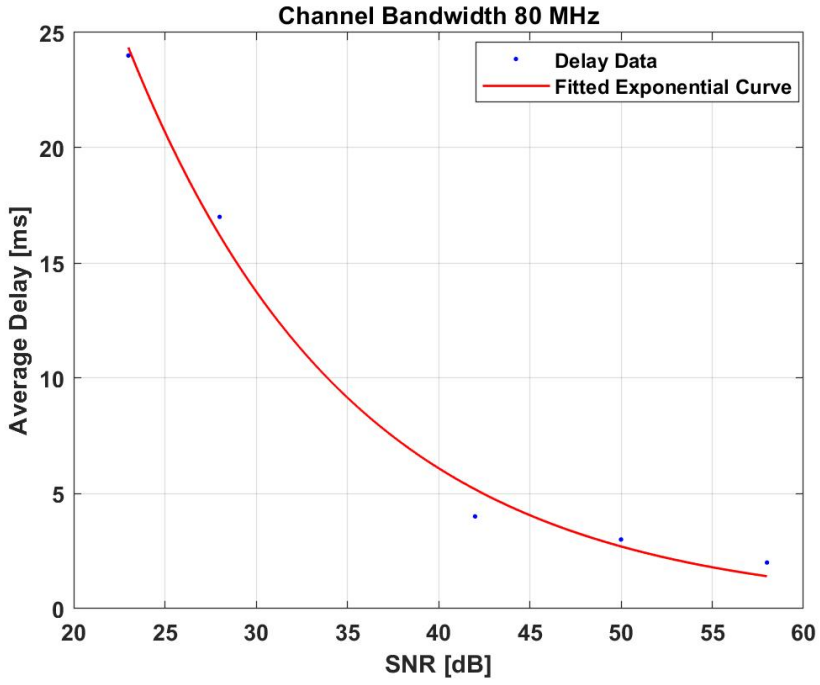

(c)

Figure 22. IEEE 802.11ac delay vs SNR model. a) 20 MHz channel width. b) 40 MHz channel width. c) 80 MHz channel width.

Discussion

The previous section presented the results of the measurement-based study performed to characterize the throughput and the delay of the IEEE 802.11ac network. The results demonstrate the following:

1. The relationship between the throughput and SNR for 3 channel width cases and two spatial streams; 20 MHz, 40 MHz, and 80 MHz; for both UDP and TCP protocols are investigated. The results show the benefit of channel bonding introduced in the standard, where the achieved throughput increased as the channel width increased. For example, for the case of UDP protocol; for an SNR value of 65 dB, the average throughput for 20 MHz channel bandwidth was around 140 Mbps as compared to 266 Mbps for 40 MHz, and 374 Mbps for 80 MHz.

   The results also demonstrate the impact of the used protocol on the maximum achieved throughput. For instance, considering the 20 MHz channel width and an SNR level of 30 dB, the throughput on average was 75 Mbps when using UDP as compared to 51 Mbps when using TCP. And this is true for all SNR levels and the three channel widths since TCP offers a reliable connection, limiting its data transmissions before requiring acknowledgments.
2. Mathematical models based on the measurements using interpolation are introduced for both UDP and TCP protocols. The calculated statistics such as RMSE and R-squared, show the accuracy of the models. For example, RMSE for the case of 80 MHz channel bandwidth when using UDP protocol was 1.372. Taking all the cases into account, the maximum RMSE was 2.1. For comparison

purposes, a mathematical model based on the Shannon's capacity theorem is presented where the Shannon's formula is modified to consider the impact of the number of spatial streams and the difference between the physical data rate and the actual achieved throughput in the transport layer of the OSI model. The results of the logarithmic model (following Shannon's theorem) show correlation of 92.8%, 89.7%, and 90.2% for the channel width of 80 MHz, 40 MHz, and 20 MHz respectively. The goodness-of-fit statistics suggests a less accurate representation of the empirical measurements using the logarithmic model as compared to the cubic spline interpolation model. The cubic spline interpolation model accurately captures and models the effect of the wireless environment on the achieved throughput while the logarithmic model is unable to represent the impact of the environment.

3. The effect of the number of spatial streams on capacity was investigated. The results illustrate the advantage of using more spatial streams as the throughput increases significantly. For instance, the throughput increases by 20% for 55 dB SNR level in the case of 80 MHz channel bandwidth and UDP protocol.
4. The results of the analysis of the relationship between the throughput of the network and the level of SIR, demonstrate the sensitivity of the throughput to the presence of co-channel interference sources. For low SIR levels (<10 dB), the interfering network dominated the channel and achieved a higher throughput. However, when increasing SIR i.e. decreasing the level of interference, the throughput of the under-test network increased and the interferer's throughput decreased.

5. The delay analysis results show that the roundtrip network delay is exponentially distributed where the delay increases as the level of SNR increases. Moreover, the results demonstrate the effect of the channel width on the delay, as the delay decreases in accordance to the increase in channel width's. The statistics show the accuracy of the model as RMSE value did not exceed 2.1 and the R-squared ranged from 0.98 to 0.99.

Chapter 5 - Conclusion and Future Work

Conclusion

The performance of the IEEE 802.11ac very high throughput standard was studied in this thesis where the impact of the channel bandwidth and the number of streams on the throughput and the delay values was evaluated. We also investigated the effect of using UDP or TCP protocols and the results showed higher throughput values for UDP compared to TCP since TCP is a handshaking-based protocol that offers reliable data exchange through acknowledgments.

An extensive measurement-based study was conducted to analyze and model the performance metrics of the 802.11ac network as a function of two important factors; SNR and SIR. Our results have shown the advantage of the enhancements provided in the 802.11ac standard. The throughput and the delay mathematical models provided in this work have very high correlation values ranging from 98% to 99% and low RMSE values ranging from 0.7 to a maximum of 2.1. These models can be used to estimate the performance of a deployed WLAN at a specific location and for a specific propagation model. A mathematical model based on Shannon's theorem was also presented to represent the throughput of the network for UDP protocol. The results of the logarithmic model showed lower correlation values as compared to the previous model and higher error values which could be linked to the lack of the quantification of the environment effect on the throughput measurements.

Furthermore, a spectral measurement tool that applies a probabilistic efficient storage algorithm PESA in real-time was presented. The algorithm is low-complex and could be used to help in the acquisition of time-domain measurements by reducing the

memory size needed to store the large number of samples obtained during long-term spectrum surveys while preserving an accurate estimation of the channel utilization and the activity temporal pattern on the channel.

The tool was developed using LabVIEW software and was tested in a healthcare wireless environment as a 7-hour survey was conducted, and the results of the survey demonstrated the objectives of the algorithm. The data storage volume was reduced by 98.8% and the error in the channel utilization error was only 1.2%. The results of this study indicate that the measurement tool could facilitate the wireless coexistence studies in different architectures and for various spectral measurements applications as it reduces the burden of using high performing computing and storage requirements.

Future work

- Introduce adaptive thresholding to the real-time PESA implementation.
- Include WLAN Packet analyzers to study other network metrics in a specific environment.
- Characterize the throughput of the IEEE 802.11ac standard when different sources of interference are present, such as LTE in the Unlicensed band (LAA, MulteFire).

References

[1] M. O. Al Kalaa, M. Ghanem, H. H. Refai, S. J. Seidman, " PESA: Probabilistic Efficient Storage Algorithm for Time-Domain Spectrum Measurements," in IEEE TRANSACTIONS ON INSTRUMENTATION AND MEASUREMENT, Forthcoming 2018.

[2] M. Höyhtyä et al., "Spectrum Occupancy Measurements: A Survey and Use of Interference Maps," in IEEE Communications Surveys \& Tutorials, vol. 18, no. 4, pp. 2386-2414, Fourth quarter 2016.

[3] T. Yucek and H. Arslan, “A survey of spectrum sensing algorithms for cognitive radio applications,” IEEE Commun. Surv. Tutorials, vol. 11, no. 1, pp. 116–130, 2009.

[4] Z. Yan, Z. Ma, H. Cao, G. Li and W. Wang, "Spectrum Sensing, Access and Coexistence Testbed for Cognitive Radio using USRP," 2008 4th IEEE International Conference on Circuits and Systems for Communications, Shanghai, 2008, pp. 270-274.

[5] C. Ghosh, S. Pagadarai, D. P. Agrawal and A. M. Wyglinski, "A framework for statistical wireless spectrum occupancy modeling," in IEEE Transactions on Wireless Communications, vol. 9, no. 1, pp. 38-44, January 2010.

[6] M. Wellens and P. Mahonen, "Lessons learned from an extensive spectrum occupancy measurement campaign and a stochastic duty cycle model," 2009 5th International Conference on Testbeds and Research Infrastructures for the Development of Networks & Communities and Workshops, Washington, DC, 2009, pp. 1-9.

[7] M. H. Islam et al., "Spectrum Survey in Singapore: Occupancy Measurements and Analyses," 2008 3rd International Conference on Cognitive Radio Oriented Wireless Networks and Communications (CrownCom 2008), Singapore, 2008, pp. 1-7.

[8] W. Balid, M. O. Al Kalaa, S. Rajab, H. Tafish, and H. H. Refai, "Development of measurement techniques and tools for coexistence testing of wireless medical devices," in 2016 IEEE Wireless Commun. Netw. Conf. Workshops, 2016, pp. 449–454.

[9] T. M. Taher, R. B. Bacchus, K. J. Zdunek, and D. A. Roberson, "Long-term Spectral Occupancy Findings in Chicago," in 2011 IEEE International Symposium on Dynamic Spectrum Access Networks, DYSPAN 2011, pp. 100-107, 2011.

[10] G. Noorts, J. Engel, J. Taylor, D. Roberson, R. Bacchus, T. Taher, and K. Zdunek, "An RF spectrum observatory database based on a Hybrid Storage System," in 2012 IEEE International Symposium on Dynamic Spectrum Access Networks, DYSPAN 2012, pp. 114–120, 2012.

[11] R. Attard, J. Kalliovaara, T. Taher, J. Taylor, J. Paavola, R. Ekman, and D. Roberson, "A High-performance Tiered Storage System for a Global Spectrum Observatory Network," in 2014 9th International Conference on Cognitive Radio Oriented Wireless Networks, CROWNCOM 2014, pp. 466-473, 2014.

[12] M. O. Al Kalaa, W. Balid, H. H. Refai, N. J. LaSorte, S. J. Seidman, H. I. Bassen, J. L. Silberberg, and D. Witters, "Characterizing the 2.4 GHz Spectrum in a Hospital Environment: Modeling and Applicability to Coexistence Testing of Medical Devices," in IEEE TRANSACTIONS ON ELECTROMAGNETIC COMPATIBILITY, VOL. 59, NO. 1, pp. 58-66, February 2017.

[13] Tianlin Wang and H. H. Refai, "Network performance analysis on IEEE 802.11g with different protocols and signal to noise ratio values," Second IFIP International Conference on Wireless and Optical Communications Networks, 2005. WOCN 2005., 2005, pp. 29-33.

[14] V. Visoottiviseth, T. Piroonsith and S. Siwamogsatham, "An empirical study on achievable throughputs of IEEE 802.11n devices," 2009 7th International Symposium on Modeling and Optimization in Mobile, Ad Hoc, and Wireless Networks, Seoul, 2009, pp. 1-6.

[15] S. Sendra, P. Fernandez, C. Turro and J. Lloret, "IEEE 802.11a/b/g/n Indoor Coverage and Performance Comparison," 2010 6th International Conference on Wireless and Mobile Communications, Valencia, 2010, pp. 185-190.

[16] Lara Deek, Eduard Garcia-Villegas, Elizabeth Belding, Sung-Ju Lee, and Kevin Almeroth, “The impact of channel bonding on 802.11n network management,” 2011, In Proceedings of the Seventh Conference on emerging Networking Experiments and Technologies (CoNEXT '11). ACM, New York, NY, USA, Article 11, 12 pages.

[17] M. D. Dianu, J. Riihijärvi, and M. Petrova, "Measurement-based study of the performance of IEEE 802.11ac in an indoor environment," 2014 IEEE International Conference on Communications (ICC), Sydney, NSW, 2014, pp. 5771-5776.

[18] D. Newell, P. Davies, R. Wade, P. Decaux and M. Shama, "Comparison of Theoretical and Practical Performances with 802.11n and 802.11ac Wireless Networking," 2017 31st International Conference on Advanced Information Networking and Applications Workshops (WAINA), Taipei, 2017, pp. 710-715.

[19] H. Alakoca, M. Karaca and G. Karabulut Kurt, "Performance of TCP over 802.11ac based WLANs via testbed measurements," 2015 International Symposium on Wireless Communication Systems (ISWCS), Brussels, 2015, pp. 611-615.

[20] Z. Shah, S. Rau, and A. Baig, "Throughput comparison of IEEE 802.11ac and IEEE 802.11n in an indoor environment with interference," 2015 International

Telecommunication Networks and Applications Conference (ITNAC), Sydney, NSW, 2015, pp. 196-201.

[21] Liao, R., Bellalta, B., Barcelo, J. et al. J, “Performance analysis of IEEE 802.11ac wireless backhaul networks in saturated conditions,” EURASIP Journal on Wireless Communications and Networking, 2013:226.

[22] S. Byeon, C. Yang, O. Lee, K. Yoon and S. Choi, "Enhancement of wide bandwidth operation in IEEE 802.11ac networks," 2015 IEEE International Conference on Communications (ICC), London, 2015, pp. 1547-1552.

[23] ITU-R, "Spectrum occupancy measurements and evaluation," SM Series Report ITU-R SM.2256, vol. 2256, no. July 2012.

[24] NI PXIe-5644R, Vector Signal Transceiver, http://www.ni.com/pdf/manuals/375880h.pdf.

[25] NI PXIe-8135, 2.3 GHz Quad-Core PXI Controller, http://www.ni.com/pdf/manuals/373716b.pdf.

[27] Eldad Perahia, Robert Stacey. *Next Generation Wireless LANs: 802.11n and 802.11ac*. 2nd ed., Cambridge University Press, 2013.

[28] https://standards.ieee.org/findstds/standard/802.11ac-2013.html

[29] https://mikrotik.com/product/RB953GS-5HnT-RP

[30] https://mikrotik.com/product/R11e-5HacD#fndtn-specifications

[31] Burden, Richard L., and J. Douglas. Faires. *Numerical Analysis*. 9th ed., Brooks/Cole, Cengage Learning, 2011.

[32] https://www.mathworks.com/help/curvefit/smoothing-splines.html

[33] L. Verma, M. Fakharzadeh and S. Choi, "Wifi on steroids: 802.11AC and 802.11AD," in IEEE Wireless Communications, vol. 20, no. 6, pp. 30-35, December 2013.

Appendix A

PESA's Implementation using LabVIEW Sub-Virtual Instruments (Sub-VIs)

1- The GMM model Sub-VI

Purpose: build the GMM model based on the dynamic range of the monitoring equipment.

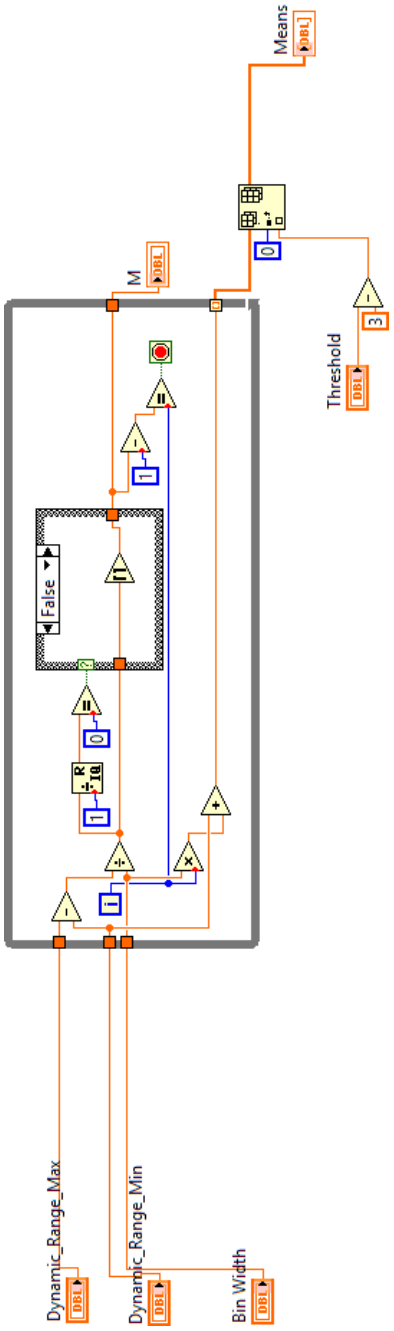

2- Activity/Inactivity Windowing Sub-VI

Purpose: establish windows of Activity/Inactivity using the raw power measurements, and find the mean and the length of each window.

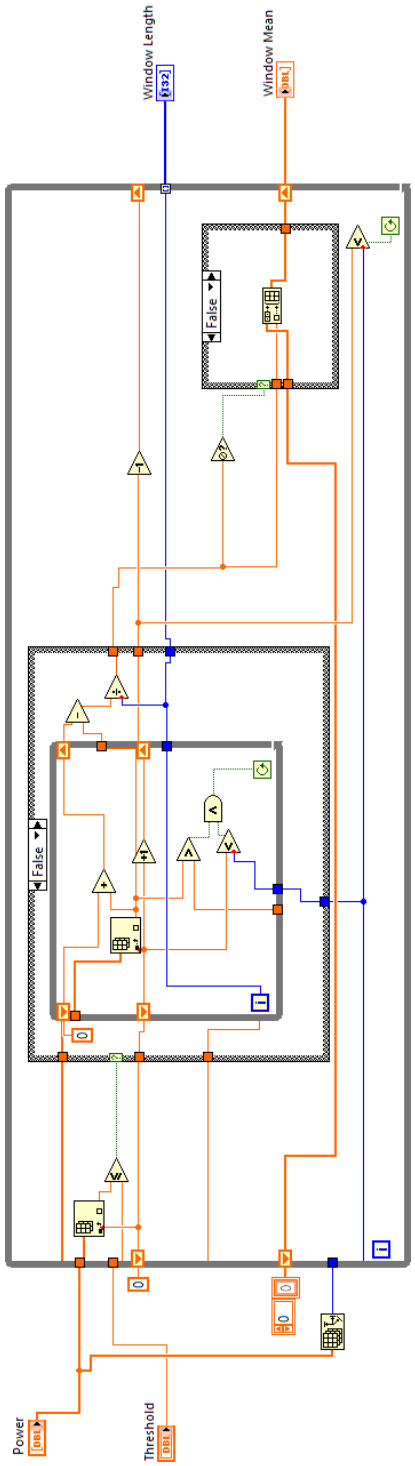

3- Finding the GMM component Sub-VI

Purpose: determine the GMM component with the highest posterior probability given the Activity/Inactivity windows' means.

